UNDERSTANDING POWER SYSTEM FREQUENCY

by

Brett Mitchell Cockerham

A thesis submitted to the faculty of
The University of North Carolina at Charlotte
in partial fulfillment of the requirements
for the degree of Master of Science in
Applied Energy and Electromechanical Systems

Charlotte

2016

Approved by:

_____
Dr. Maciej Noras

_____
Dr. Bogdan Kasztenny

_____
Dr. Sukumar Kamalasadan

ABSTRACT

BRETT MITCHELL COCKERHAM. Understanding power system frequency (Under
the direction of DR. MACIEJ A. NORAS)

Frequency of an electrical signal is defined during steady state conditions,

although it can be problematic to measure. However, power system frequency can often

fluctuate during power swings and other anomalous events. These events can be

characterized as non-periodic signals where frequency is not generally defined [1]. In

industry, phasor measurement units (PMU) are used by utility companies to measure

voltage and current in the power system. These digital samples obtained from the PMU

are included within an algorithm where phasors and frequency of the power system are

computed. To report these values with desired accuracy, the frequency of the system

must be well known. The PMU's are often subjected to varying signal types and

depending upon the implemented algorithm the computed fundamental frequency

component can vary [2, 3]. These signal types are, but not limited to: phase modulated,

amplitude modulated, phase angle step, magnitude step, frequency ramp, harmonics,

inter-harmonics, etc. These signal types may lead to discrepancies between fundamental

frequency values reported by different PMUs processing the same signals measured from

the power system. This demonstrates that an advanced understanding of frequency needs

to be addressed.

The study was conducted to determine the inconsistency between PMUs sold by

different manufacturers. To determine if there is an underlying inconsistency between

multiple PMU manufacturers, tests were performed to provide insight into the

implemented guidelines stated within IEEE std. C37.118.1a-2014. Four compliant PMU

devices were subjected to several signal types listed within the IEEE standard. To ensure

the implemented frequency method is robust, dynamic events must be considered so that

they also measure the fundamental frequency accurately when subjected to varying signal

parameters. The maximum reporting difference, via IEEE std. test events, was 72.6 mHz.

However, a frequency excursion event captured on the power system was replayed to

each of the devices and the reported fundamental frequency values differed up to 748.3

mHz in some instances. This is an order of magnitude greater for the real system event

versus the IEEE std. test conditions. In addition to testing the four individual PMU

devices and alternative frequency estimation method is proposed.

The new proposed frequency method was designed to be fast and accurate for

varying signal conditions. The new method allows for frequency reporting at the same

rate as the sampled signal. The method was tested for accuracy and compliance using the

same test signals defined by the IEEE std. C37.118.1a-2014. For the tested signal

conditions, the frequency method resulted in error as little as 0.8 mHz for steady state

signals and yielded a maximum error of 49.1 mHz for a phase modulated signals. The

test results showed that the new proposed frequency method was compliant with the

IEEE std. C37.118.1a-2014 for all tested signal types.

ACKNOWLEDGMENTS

College professors can play a huge influential role in students and their success during college. I have had the honor of being a student to many great professors throughout my college experience. One professor that made an influential impact on my college studies is my adviser Dr. Maciej Noras. I'd like to thank him for his contribution and support throughout this research and my education. Dr. Noras has encouraged me to strive for more since the beginning of my undergraduate studies. Thanks again for the time, expertise, support, advice, and guidance you have given me on so many occasions Dr. Noras.

I'd like to thank Dr. Bogdan Kasztenny for introducing this topic to me. I instantly became intrigued to learn more about the challenges of measuring frequency when he suggested the research for my thesis. Thank you for your time and continuing to provide feedback throughout this research. Your knowledge and guidance is greatly appreciated. Frequency will continue to be a topic that I will always enjoy.

I also would like to thank my committee for the many meetings they participated in, along with reviewing this document. I would also like to thank Dr. Sharer for her time and effort in proof reading this thesis. Many thanks to all professors that have taught me over the years. Thank you to all of the participating PMU manufacturers.

Lastly, I would to thank all my family and friends that continued to provide encouragement throughout my entire education.

TABLE OF CONTENTS

CHAPTER 1: INTRODUCTION

In power systems synchronous generators are traditionally used as the means of converting mechanical energy to electrical energy [4]. This is accomplished by turning the generators rotor which consist of a field winding connected to a direct current source; this induces an electromotive force (EMF) into a stationary winding. The induced EMF is comprised of three phase alternating voltages. The fundamental frequency component of these voltages generated are directly related to the speed of rotation of the generator rotor [5].

Conventional generation has a significant amount of inertia associated with a large rotating mass. Due to this inertia, the large rotating mass cannot change abruptly. This would imply that the fundamental frequency component of the induced voltage signals doesn't change abruptly since the electrical frequency is directly related to the rotors rotational speed. However, electrical signals are affected differently by other factors such as: faults and switching transients, which could result in rapid changes in the signal. Therefore, the electrical definition of frequency continues to be challenged due to many events that can abruptly change the electrical signal. The events consist of, but not limited to: phase modulations, frequency ramps, magnitude steps, and phase angle steps.

In the power system, there are phasor measurement units (PMU) that are installed in various locations that measure both voltage and current signals. In PMUs, the fundamental frequency is estimated using the measured voltages or current signals.

There are a broad variety of signal processing algorithms that are employed within the phasor measurement units (PMU) to calculate the systems fundamental frequency such as: the zero-crossing method, adjustment points method, recursive based discrete Fourier transform, etc. The performance of each method can vary depending upon the systems conditions. Due to the variance of frequency algorithms and no common definition in industry, PMUs can yield different values for frequency. Four PMUs were obtained for frequency measurement comparisons to determine if there is any inconsistency between manufactures when subjected to various event types (e.g. steady state, phase modulated, amplitude modulated, frequency ramp and input step waveforms). For an additional analysis, a real power system frequency excursion was replayed to each of the PMUs to further outline if any difference in reported frequency could occur. Each tested PMU is compliant with the IEEE std. C37.118.1a-2014. The IEEE standard does not give a specific frequency method to use it only specifies performance guidelines for frequency measurements when subjected to the various event types. There are two performance classes: M- and P-class. The IEEE std. C37.118.1a-2014 defines the classes as [6, 7],

"P class is intended for applications requiring fast response and mandates no explicit filtering. The letter P is used since protection applications require fast response.

M class is intended for applications that could be adversely effected by aliased signals and do not require the fastest reporting speed. The letter M is used since analytic measurements often require greater precision but do not require minimal reporting delay."

The PMUs were tested using M class with a reporting rate of 60 frames/sec.

Another goal of this research is to develop a frequency measurement method that responds fast and accurately throughout the various events encountered on the system. There is often a tradeoff between fast and accuracy for frequency measurement techniques. Accuracy, in most cases, requires extensive pre- and/or post-filtering; however, filtering adds unintentional delay and slows the response of the measurement method. The proposed method is to update the value of frequency with each new sample obtained from the algorithm, this allows for increasing the reporting rate of frequency. Lastly, the new method will be compared against the four PMUs to verify performance and accuracy.

CHAPTER 2: LITERATURE REVIEW

2.1 Overview of Power System Frequency

The power system includes multiple generators and various loads interconnected at any given point in time. This would suggest that the power system is in a continuously changing state [8]. With generators and loads being sensitive to system frequency [9], there is a need for actions to ensure power system fundamental frequency is maintained. In addition, not only are generators and loads sensitive to equipment, a decrease in frequency could lead to a system collapse. This would result in a blackout in the interconnected area. With electricity heavily relied upon, maintaining system stability levels is essential. Various techniques to ensure the system is maintained at an operable state (nominal frequency and voltage) are discussed. This chapter discusses the importance and methods of measuring the fundamental frequency for three phase AC voltages and currents throughout the power system.

2.1.1 Power System Stability

There are two categories that are widely agreed upon to categorize power system stability issues: transient instability and oscillatory instability [10]. The Power Engineering Society (PES) defines transient instability when a fault and/or switching event occurs [10]. A transient implies a sudden change between two steady state conditions. When a fault occurs, a significant amount of current is supplied to the fault location. This level of current often subjects the system to huge mechanical and thermal

stresses that need to be diminished to maintain safety, health of the equipment, and

system stability [10]. To prevent excessive periods of transient instability, quick event

monitoring and rapid circuit breaker operation is necessary. Oscillatory instability

categorizes the natural oscillation frequency of the power system [10]. When a physical

system is not properly damped, oscillations can occur around the operating point until

steady state conditions are satisfied [10]. PES defined two levels of oscillatory instability

behavior: local mode oscillations (1-2Hz) and inter-area oscillations (0.1-0.6Hz).

Transient instability could lead to oscillatory instability if the fault occurs on an essential

transmission line. Luckily, dynamic oscillations are typically contained due to the natural

damping effects associated with the system. When the system is no longer able to

provide adequate damping, voltage regulators and/or power system stabilizers can be

added to the system. Both of which add negative damping to the power system to

remove the oscillations. The principle operation of a voltage regulator is to alter the

excitation level of the generator and to maintain terminal voltage [10]. Power system

stabilizers detect changes in frequency, power, and shaft speed. The concept is to send an

external signal to the voltage regulator to modify the damping level. This illustrates the

need for an accurate frequency measurement and with variance of computational

methods, the reported fundamental frequency can vary.   In addition to transient and

oscillatory instability, another method to maintain power system stability is referred to as

automatic gain control (AGC).

2.1.2 Automatic Gain Control

The generators and loads interconnected to the power system are sensitive to

system frequency [9]. When there is a mismatch between power generation and load, the

system frequency can increase or decrease [8-15]. If a significant generating source is suddenly tripped (disconnected from the system), the system initially has a large loading on the connected sources. This initial loading will first be compensated by the kinetic energy stored in each of the large rotating rotors within the system, but once the inertia is exhausted, frequency will begin to decline [9]. As the fundamental frequency decreases, the loads power consumption will also decrease. Jaleeli et al. [9] note that larger systems can often recover independent from external control, if the system is not restored within two seconds, external control is necessary. External controls can be manual or automatic. AGC will increase the speed of the generator in order to restore the nominal system frequency [9]. This automated process can reduce response time in as little as 1-2 minutes. The response time is based on the physical limitations of the equipment and processing time of the controller [9]. The AGC is expected to maintain the generator frequency within predefined limits. In the slight chance that the AGC is unable to recuperate the system frequency within the limits, the operation is switched to manual control. The time of frequency restoration is dependent on the level of urgency [9]. A system collapse can occur if the frequency is not recovered in time. To prevent system collapse load shedding schemes are often employed [8, 12-15].

2.1.3 Load Shedding

Load shedding is the absolute last resort as an attempt to restore system frequency [4-8]. Load shedding involves disconnecting a portion of the load to restore the balance between generation and load. However, there are two distinct types of load shedding: under-frequency load shedding (UFLS) and under-voltage load shedding (UVLS) [13, 14]. As stated by Hoseinzadeh et al. [13], the concepts of UFLS and UVLS show to be

independent of each other; however, they both can have a single cause. An under-voltage event is identified as a local area phenomenon and as distance is increased from the point of incident, the voltage is closer to the nominal value. UVLS is usually required where lack of reactive power is provided to the load [13, 14]. Under-frequency is an event that is global, meaning the entire interconnected system is affected. However, Hoseinzadeh et al. [13] suggest that under-voltage and under-frequency events should be coordinated as one. The load shedding devices record the voltage data to determine the frequency, and combining the two sets of information allows both to be considered simultaneously. In [12-14], the principles and guidelines for load shedding are discussed. Load shedding parameters were also established. To determine how to employ various levels of load shedding, the frequency thresholds must be defined, the load shed amount (power) should be declared, and intentional time delays should be established. The latter will prevent from random load shedding across the network due to differences in frequency at any given location [12].

2.1.4 Frequency at Steady-State

In electrical engineering frequency is generally considered when evaluating either a current and/or voltage signal. An electrical signal, containing a signal frequency component, is mathematically represented as follows [16]:

$$v(t) = V\sin(2\pi f t + \Theta) \tag{1}$$

Where: $v(t)$ = time dependent sinusoidal waveform

V = amplitude voltage

f = frequency (Hz)

Θ = phase shift (rad)

$$2\pi f = \text{angular velocity (rad/s)}$$

Equation (1) can be expressed graphically by plotting time versus voltage.
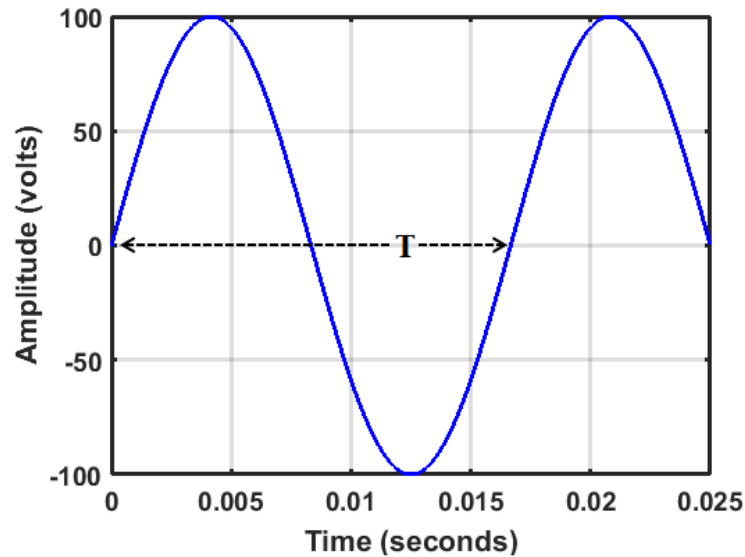
Figure 1: Time versus voltage

Using Figure 1 as a visual aid, in conjunction with the prior definition of

frequency "rate of occurrence", the frequency can be determined by measuring the

minimum time at which the signal re-occurred. In this case "T", denoting the period, is

the time where the signal starts to replicate itself (estimated to be $0.01\bar{6}$ seconds in Figure

1). This is described mathematically below [17]:

$$x(t) = x(t - T) \tag{2}$$

Frequency is most defined using the units of Hertz (Hz), and the conversion

from time in seconds to Hertz can be achieved using the following equation:

$$f = \frac{1}{T} \tag{3}$$

Using Equation (2) and the measured time of $0.01\bar{6}$ seconds, the frequency of the

signal illustrated in Figure 1 is 60 Hz.

In Figure 1, a single sinusoidal waveform is presented; however, in power systems three signals are simultaneously present and is referred to as a three-phase system. A set of balanced three-phase voltage signals can be expressed by applying the appropriate phase shift to Equation (1).

$$v_A(t) = V\sin(2\pi ft) \tag{4}$$

$$v_B(t) = V\sin(2\pi ft - 120°) \tag{5}$$

$$v_C(t) = V\sin(2\pi ft - 240°) \tag{6}$$

Equations (4), (5), and (6) are labeled with a corresponding subscript letter, denoting the phase. The waveforms are superimposed on the following graph:
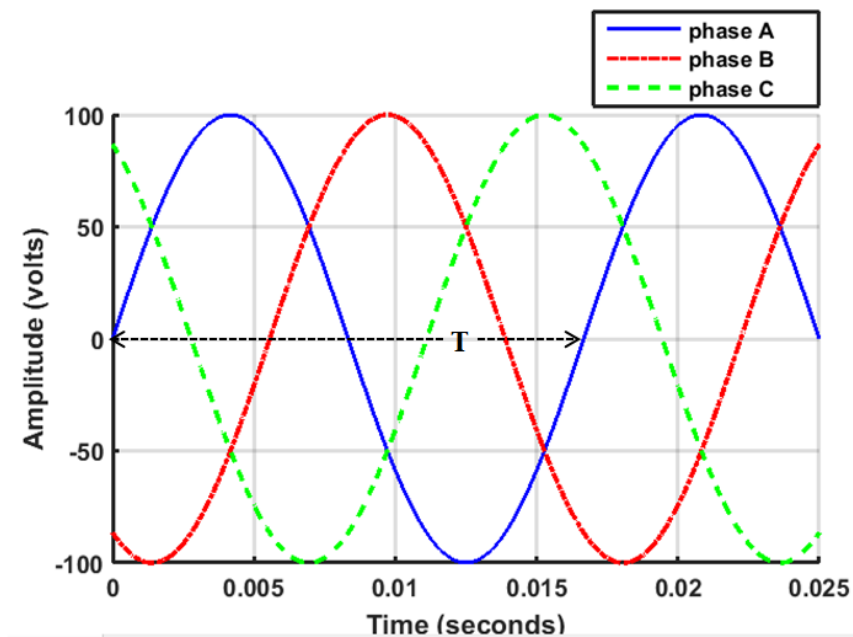

Figure 2: Three phase, time versus voltage

As described by Equation (2), the frequency of phase A is the inverse of the time where the signal replicates itself. One thing to note is that phase B and phase C will yield the same frequency result as of phase A.

2.2 Frequency Measurement Challenges

Since the invention of AC machines frequency measurements have been widely employed throughout power systems [5]. Traditionally, there were mechanical devices where resonance-type frequency metering was applied [5]. Hardware based zero-crossing detectors followed. With the advent of microprocessor based relays, frequency is now measured using signal processing techniques. Even with the evolution of technology, the power industries interpretation of measured system frequency continues to be challenged [17]. Various dynamic signal types, signals containing harmonics and inter-harmonics, and input step changes impose difficulty on the signal processing techniques implemented in industry today.

2.2.1 Dynamic Signals

AC frequency is well-defined for steady-state signals; however, the power system is continuously changing and fluctuating. In most cases the system frequency stays in a narrow range from a nominal value (50Hz or 60Hz), ± 0.5 Hz, but there are disturbances that could lead to frequency departures up to ± 10 Hz [5, 18]. Two dynamic signal types are modulated waveforms and signals with a ramp in frequency.

2.2.1.1 Modulated Signals

One form of frequency disturbance is created from incorporating multiple AC generators on the grid. With the interconnection of AC generators on the system, modulated signals could be created [5, 18]. The connection of multiple generators, all at slightly different speeds, create a superposition of voltage and currents with frequencies that differ. This could result in an oscillatory system frequency ranging from 0.1-10 Hz [5]. Both amplitude and phase angle modulations could occur simultaneous or

independent of each other [5, 18]. An amplitude modulated waveform does not vary the fundamental frequency; it however modulates the amplitude of the signal. The figure below displays an amplitude modulated signal:
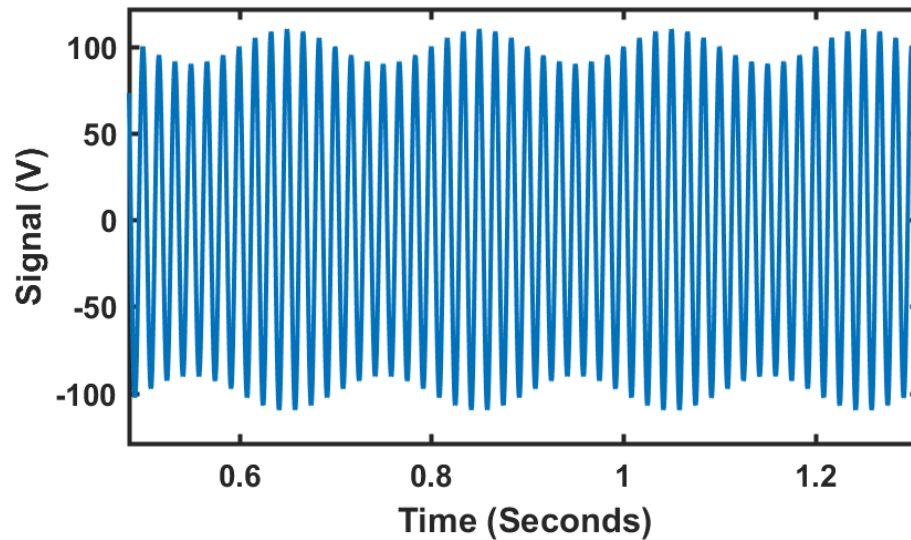
Figure 3: Amplitude modulated signal

As previously described in Equation (2), ideal sinusoidal steady state signals are consistent in amplitude and frequency (therefore in period). The amplitude modulated waveform will not change the time between zero-crossings that define the period, but this signal type will not comply with the definition provided by Equation (2) where two successive cycles must be identical in amplitude.

The next modulation type is phase angle, and an example of the time response for this signal classification is shown in Figure 4:
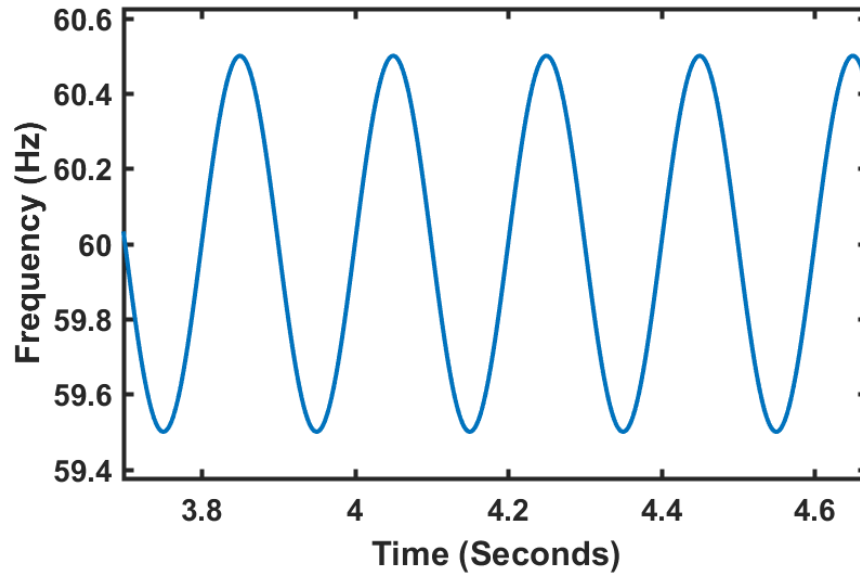
Figure 4: Phase angle modulated signal

The y-axis on the plot is now the system frequency. The phase modulated signal varies the fundamental frequency component at an oscillatory rate. Measuring the erratic changes in frequency can be problematic to any frequency determination method.

2.2.1.2 Frequency Ramp

Recall that the frequency of the voltage and current signals is proportional to the speed of rotation of the generator. Changes in the frequency response of the generator can occur because of mismatch between generation and load [5]. For instance, if the generator is operating at full capacity and suddenly a large portion of load becomes disconnected then the frequency could increase in a ramp fashion. Due to the inertia of an electrical machine the rotor cannot abruptly change its rotational velocity, in a step fashion, from one steady-state value to another. A sudden loss in load could occur when a transmission line was disconnected from the source due to a fault. Similarly, if the load requires more power than generated power available, the speed of rotation would decline, thus the frequency also declines. A plot for a linear frequency ramp is shown below:
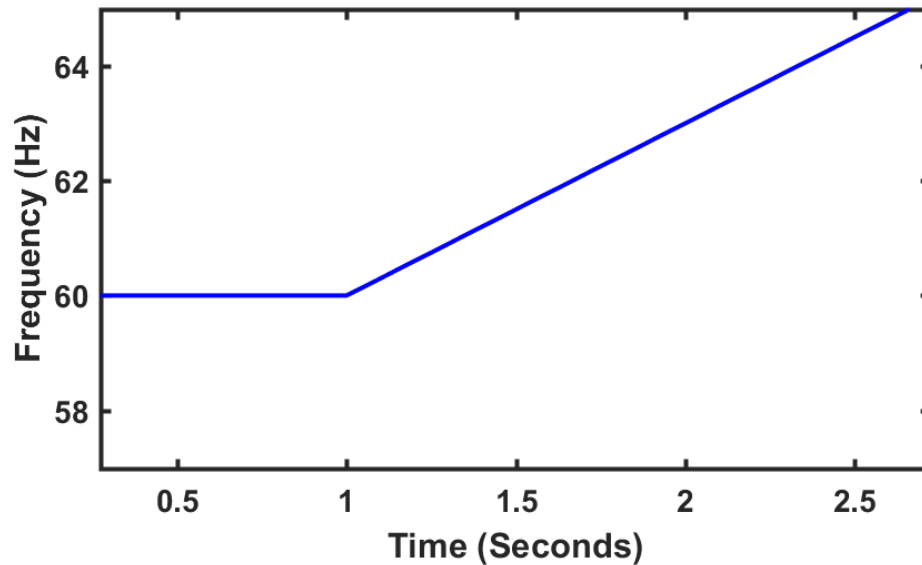
Figure 5: Frequency ramp signal

Figure 5 shows a steady state signal of 60 Hz and, at one second into the plot, the frequency increases at a linear rate. When a frequency ramp occurs, just as any other source of frequency deviation, two successive cycles don't necessarily have to be identical.

2.2.2 Harmonics and Interharmonics

Harmonics and inter-harmonics create waveform distortion. Harmonics are frequencies that are superimposed on a signal where the frequency is an integer multiple of the fundamental [19]. For instance, for a 60 Hz fundamental system the 2nd, 3rd, and 4th harmonic would be 120, 180, and 240 Hz respectively. In [19], it's listed that typical harmonics range from 0-100 with a magnitude of 0-20% of the fundamental component. Inter-harmonics are harmonics that are not integer multiples of the fundamental frequency (e.g. multiples of 2.1, 4.73, and 8.2) [19]. Inter-harmonics could potentially create issues when determining frequency. When they are superimposed on a fundamental frequency, one cycle will not precisely overlay the cycle that immediately follows even during the steady state. Because of this nature, inter-harmonics can

challenge any frequency measurement method. Inter-harmonics could typically occur

between 0-6 kHz with a magnitude of 0-2% of the fundamental [19].   Both harmonics

and inter-harmonics are due to the nature of nonlinear loading on the power system [19]

and the level of harmonic/ inter-harmonic experienced, in addition to the harmonic

multiple, is dependent on the connected load and/or fault type. Power electronics,

induction motors, and arcing devices are few examples of sources that create harmonic

distortion [19].

2.2.3 Magnitude and/or Phase Angle Step

Steps in magnitude or phase angle steps are artifacts of switching events and/or

faults on the system [5, 18]. They can occur simultaneously or as a combination

depending upon the system conditions. These scenarios challenge any interpretation or

definition of power system frequency [5, 17, 18]. Below illustrates a step-in phase:
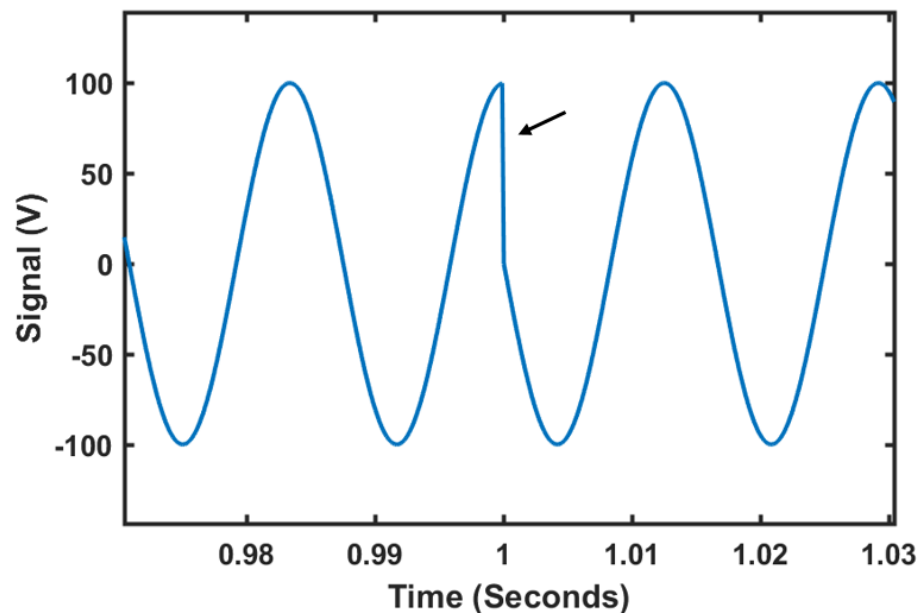
Figure 6: Phase angle step signal

The arrow in the above figure denotes a phase angle step in the measured signal.

This step creates a discontinuity in the waveform which creates high frequency

components. This skews many or all algorithms used to determine frequency. Another form of an input step signal is shown below:
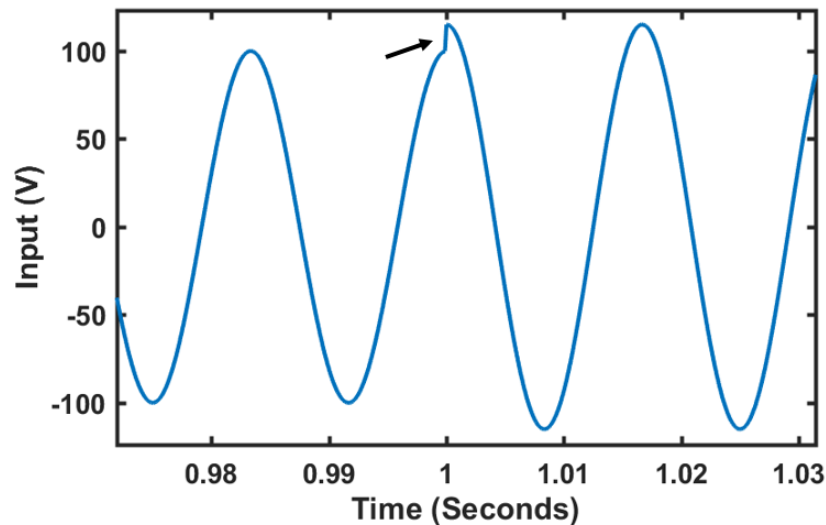
Figure 7: Magnitude step signal

The figure above shows a steady state signal that rapidly changes from one voltage level to another when time = 1 second. The fundamental frequency never alters for this signal; however, depending upon the implemented frequency measurement method, the reported value will change.

2.3 Review of Power System Frequency Measuring Methods

A few of the measurement challenges for determining the power systems frequency have been reviewed in the previous section. The following section reviews signal processing techniques for determining the power system frequency.

2.3.1 Techniques for Measuring AC Frequency

With the advent of digital microprocessors, several digital methods have been implemented to estimate the value of frequency in the power system [20]. Digital measurement devices are connected to the system through instrument transformers that step-down levels of voltage and current. Voltages and currents on the power system are

continuous in time. The digital measurement device takes discrete samples in time from

this signal. The digital methods use the digital discrete samples to calculate frequency.

Three widely accepted methods will be discussed; however, there are many more

algorithms available. The three frequency estimation methods reviewed are zero-

crossing, the adjustment point method, and the discrete Fourier transform (DFT).

2.3.1.1 Zero-crossing Method

A popular method of estimating frequency is using zero-crossing detection [21].

This method offers an easier approach compared to many other frequency estimators

available. The zero-crossing method is derived from the measurement interval of time

between two zero crossings of a signal. For instance, Figure 8 shows a single-phase

voltage signal with discrete measurement values graphed. The discrete values are the

only information that can be obtained through sampling, therefore any information from

an event between the samples is lost. This is simply an artifact of using an analog to

digital converter (ADC). When using an ADC with a fixed clock, each sample obtained

is separated by the same amount in time, this time can easily be determined by knowing

the rate at which the samples were obtained. This is referred to as the sampling

frequency.
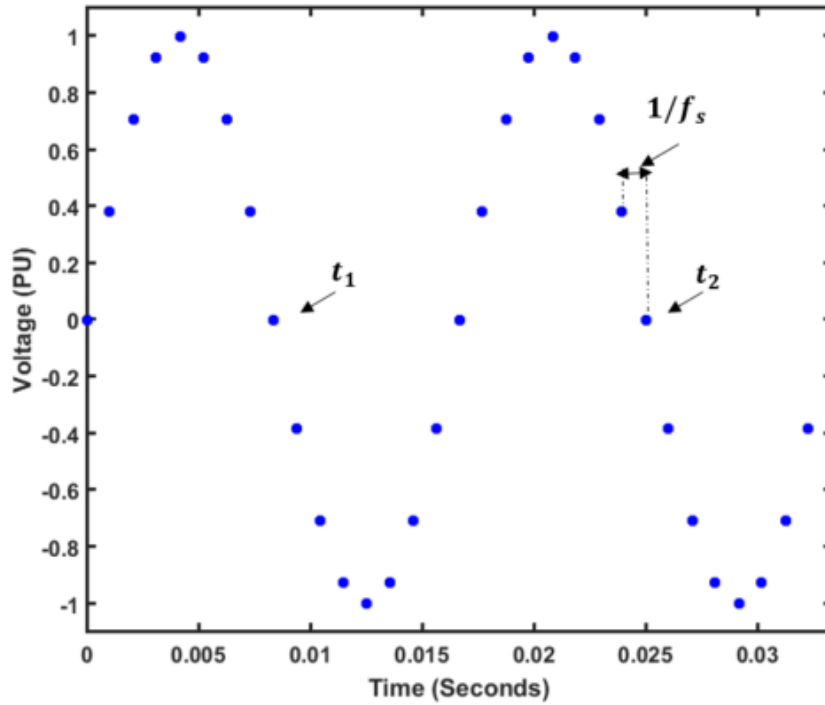
Figure 8: Sampled voltage signal

The signal's fundamental frequency in Figure 8 can easily be determined by knowing the time interval between zero crossings. A generic form of the zero-crossing method can be described using the following equation:

$$F(t_M) = \frac{(M-1)}{2} \times \frac{1}{t_M - t_1}$$ (7)

Where: F = estimated frequency value

M = number of zero crossings within the data window

t_M = time of the most recent zero crossing

t_1 = time of the first zero crossing in the data window

Equation (7) is a general form of a zero-crossing measurement method. It looks at every zero crossing that occurs. Evaluating each zero crossing to determine a frequency estimate can only be accurate when the waveform contains odd-symmetry; however, any measured periodic signal does not have to have this odd-symmetry. If there

is any slight DC offset in the measured signal, Equation (7) could yield an incorrect

frequency value. In [19], it is reviewed that a DC offset could be present in the AC

power system due to geomagnetic disturbances. Typical values range from 0-0.1% of the

voltage magnitude [19] and is illustrated in Figure 9, which includes a measured voltage

signal that includes a DC offset.
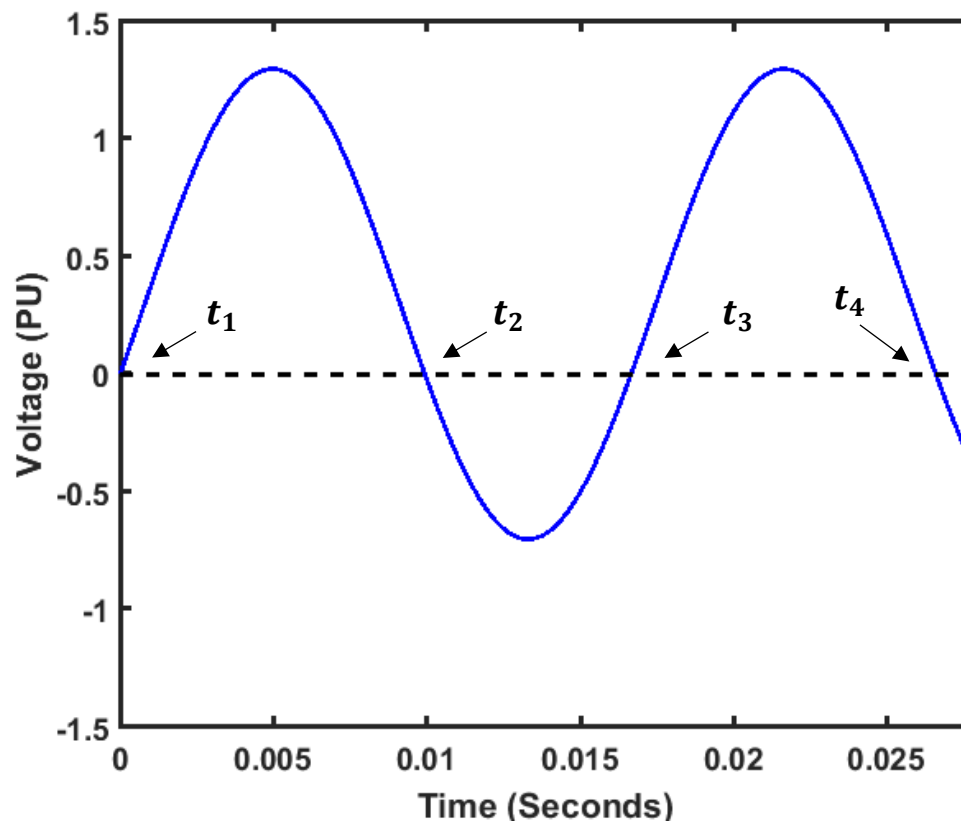
Figure 9: 60 Hz voltage signal with DC offset

Notice in Figure 9 that the 60Hz signal remains positive for a longer duration than

that of the negative portion of the waveform. This relationship removes the odd-

symmetry about the x-axis. To see the effect of DC offset and the impact of Equation (7)

in the evaluation of frequency, Table 1 represents the time at which each zero crossing

occurs, along with corresponding frequency estimation values for each time interval.

Table 1: Effects of DC offset on the zero-crossing method

Sample	DC Offset		DC Offset Removed	
	Sample Time (ms)	Measured Frequency (Hz)	Sample Time (ms)	Measured Frequency (Hz)
t_1	0	-	0.808	-
t_2	9.949	50.252	9.141	60.000
t_3	16.667	60.000	17.474	60.000
t_4	26.616	56.356	25.808	60.000

When using the time of zero crossings for the 60 Hz signal in Figure 9, Equation (7) yields large errors for the estimated frequency when a DC offset is present. This demonstrates that this method is severely impacted by the DC offset. For this reason, some zero-crossing methods evaluate the zero-crossing event from positive-to-negative sample values and others evaluate from negative-to-positive [17]. Either of the two could be implemented using a modified version of Equation (7) displayed below:

$$F = (M - 1)\times \frac{1}{t_M - t_1} \tag{8}$$

Equation (8) is similar to Equation (7), but the two was removed to evaluate an entire cycle instead of half-cycle. This equation is valid when evaluating positive-to-negative or negative-to-positive sampled zero crossings. This is demonstrated in the figure below:
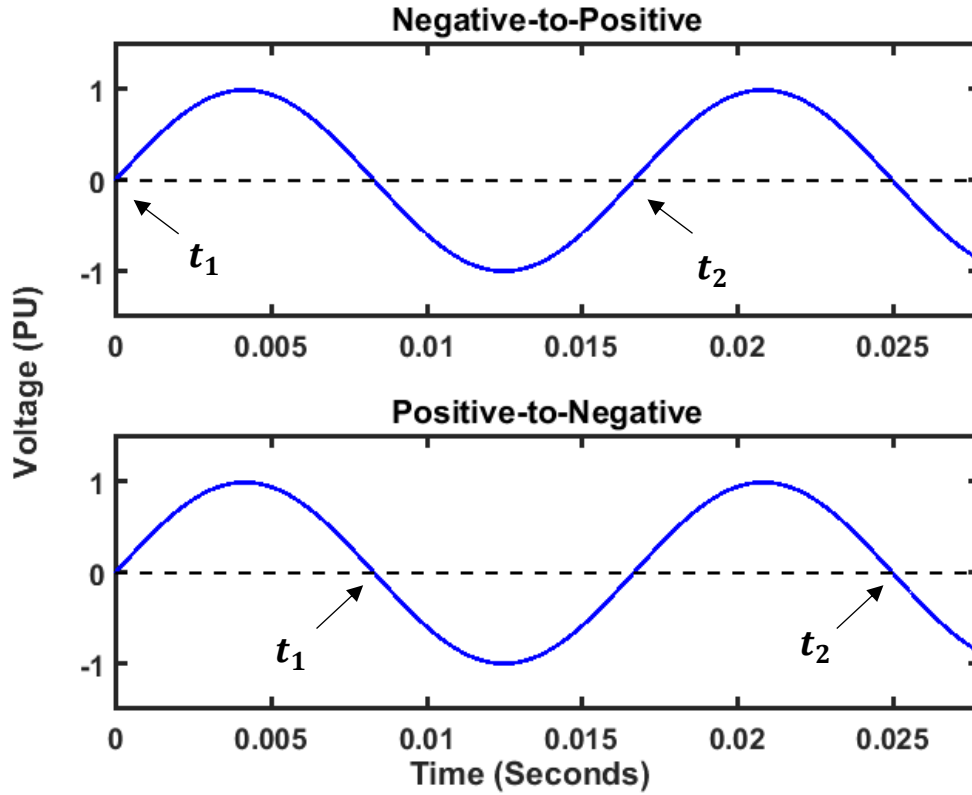
Figure 10: Negative-to-Positive vs. Positive-to-Negative

Figure 10 illustrates which zero crossings are evaluated for Equation (8) based on either of the two methods presented. The signal in Figure 9 was evaluated for 44ms to obtain more zero crossings, using the zero crossings obtained Equation (7) and (8) are compared in the table below:

Table 2: Comparison of Equation (7) and Equation (8) with DC offset

Sample Time (ms)	Equation (7)		Equation (8)	
	Sample	Measured Frequency (Hz)	Sample	Measured Frequency (Hz)
0	t_1	-	t_1	-
9.949	t_2	50.252	-	-
16.667	t_3	60.000	t_2	60.000
26.616	t_4	56.356	-	-
33.333	t_5	60.000	t_3	60.000
43.283	t_6	57.759	-	-

Table 2 shows that Equation (8) removes the effect of DC offset if the offset is constant for the duration of the evaluated window. One thing here is, if the DC offset was not present then both methods would work equally well but Equation (7) would update the value of frequency with each new zero crossing. However, Equation (8) will only update the value of frequency every other zero crossing.

Harmonics can often be present in power system voltages and currents; this could have devastating effects on the zero crossing methods discussed [17]. For instance, the figure below illustrates a heavily distorted voltage signal, degraded with harmonics:
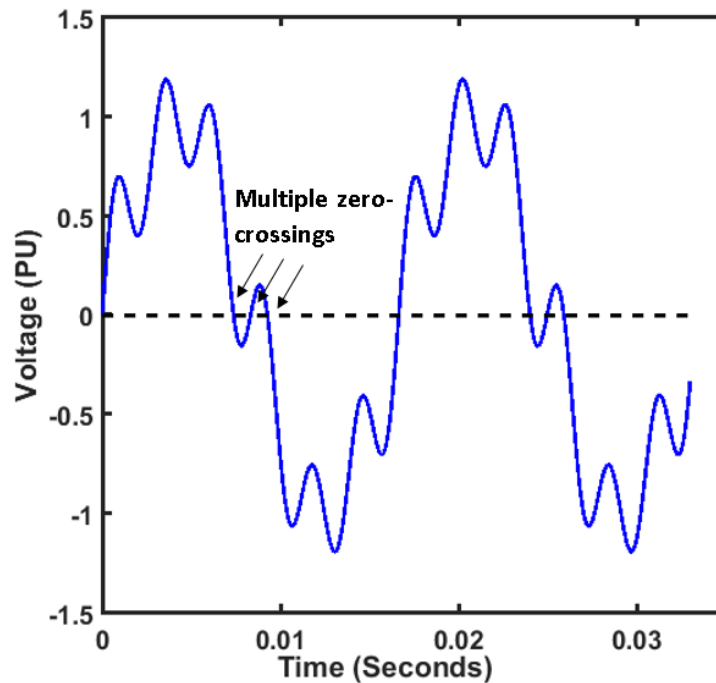
Figure 11: Distorted voltage signal

Figure 11 shows how harmonics could affect the zero-crossing method. Either of the zero crossing methods would easily be corrupted and yield false frequency estimations. For this reason, pre-filtering is required to ensure that events like this are not measured by the PMU [22].

Another issue with the zero-crossing method is that the sampled value of the signal will unlikely be exactly at zero. For each zero crossing event to land exactly at zero, the sampling frequency (f_s) would need to be an integer multiple of the fundamental frequency [23]. To account for this issue, geometrical relationships can be incorporated to determine an approximation for the time at which the zero-crossing occurred. There are several interpolation methods to achieve high accuracy for these instances. In [21], three interpolation methods were investigated for the zero crossing method specifically. The three methods inspected are linear, quadratic, and cubic interpolation. Cubic interpolation performed the best, followed by linear and then quadratic; however, in practice linear interpolation is typically the chosen due to the minimal processing requirements [21]. Figure 12 illustrates why interpolation is necessary in the determination of frequency in a zero-crossing technique:
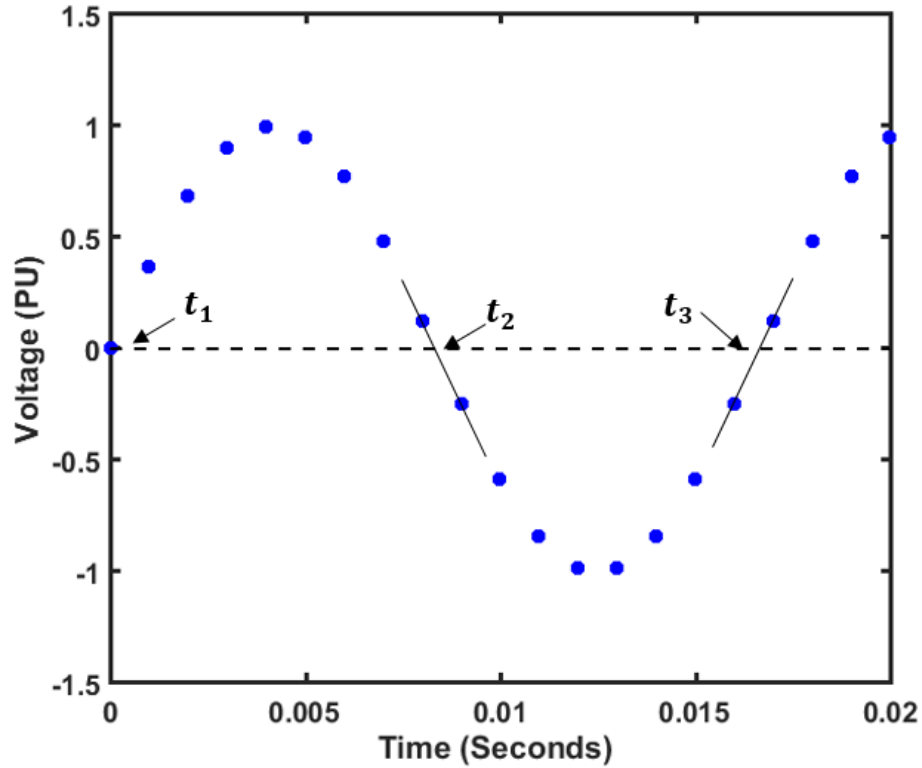
Figure 12: Sampled voltage signal to determine time of zero crossings

As mentioned previously, if the sampling frequency is not an integer multiple of the fundamental frequency (which may be variable), it is unlikely that the measured sample will be zero during a zero-crossing event. This is demonstrated in Figure 12 where the sampling frequency is 1 kHz and the fundamental frequency of the signal is 60 Hz. The time at which each sample in the graph is shown can be determined by knowing the sampling frequency and the sample number. To find the approximated time of the zero crossing it requires more than taking the average of the two samples [17]. You must interpolate the value for a closer approximation, this is where interpolation is very effective. One form of linear interpolation is shown in the equation below:

$$t_k = \frac{[V_k - V_{k-1}] \cdot [t_{k+1} - t_{k-1}]}{V_{k+1} - V_{k-1}} + t_{k-1} \tag{9}$$

Where: t_k = time of zero crossing

$$V_k = \text{zero}$$

$$V_{k-1} = \text{sample value before zero crossing}$$

$$V_{k+1} = \text{sample value after zero crossing}$$

$$t_{k-1} = \text{sample value occurrence time before zero crossing}$$

$$t_{k+1} = \text{sample value occurrence time after zero crossing}$$

The table below uses Equation (9) to determine the time at which the zero crossing occurs. In addition, the table includes the average of t_{k+1} and t_{k-1} to compare with the linear interpolation accuracy.

Table 3: Linear interpolation vs. averaging samples to find the time of zero crossing

	Linear Interpolation (ms)	Accuracy (Hz)	Average (ms)	Accuracy (Hz)
t_1	-	-	-	-
t_2	8.335	0.012	8.500	1.176
t_3	16.665	0.006	16.500	0.606

Table 3 above illustrates the effectiveness of linear interpolation in Equation (9) and how taking the average of the two sample times on each side of the zero crossing doesn't accurately depict the time of zero crossing.

2.3.1.2 Adjustment Points Method

The adjustment points method is far different from the previously mentioned zero crossing. A rudimentary version of the adjustment point method is explained in [21]. The method computes frequency from using three consecutive sample points. Considering a sinusoidal signal as defined in Equation (10) [21]:

$$v_k(t_k) = X_m \sin(2\pi f k t_s + \alpha) \tag{10}$$

Where: f = fundamental frequency of the sinusoidal signal (Hz)

X_m = Amplitude of the measured signal

k = sample number

t_s = interval time between samples, also equal to $1/f_s$ (s)

t_k = time at which sample k was obtained, also equal to $k \cdot t_s$ (s)

v_k = sample value obtained from signal

α = phase shift (radians)

Equation (10) characterizes the sample obtained from the signal. Assuming a constant phase shift, the two samples followed by sample v_k can be represented as [21]:

$$v_{k+1}(t_k + t_s) = X_m \sin(2\pi f(kt_s + t_s) + \alpha) \tag{11}$$

$$v_{k+2}(t_k + 2t_s) = X_m \sin(2\pi f(kt_s + 2t_s) + \alpha) \tag{12}$$

Where: $\quad v_{k+1}$ = first sample value obtained after v_k

v_{k+2} = second sample value obtained after v_k

Once Equations (10) and (12) are summed, Equation (11) is substituted in and the yielding updated equation is [21]:

$$\cos(2\pi f t_s) = \frac{v_k + v_{k+2}}{2v_{k+1}} \tag{13}$$

Equation (13) can be modified to solve for the frequency, as shown below:

$$f = \frac{1}{2\pi t_s} \cos^{-1}\left(\frac{v_k + v_{k+2}}{2v_{k+1}}\right) \tag{14}$$

Equation (14) yields the adjustment point method also referred to as the three-point method, considering frequency is estimated using only three samples of a waveform. The method essentially estimates the instantaneous frequency of a sinusoidal signal. The benefit of instantaneous frequency estimation is that frequency can be computed on demand and doesn't rely on a specific event (e.g. zero crossing). One issue

with Equation (14) is the estimated frequency yields large errors when denominator

$2v_{k+1}$ is close to zero; this is illustrated below:
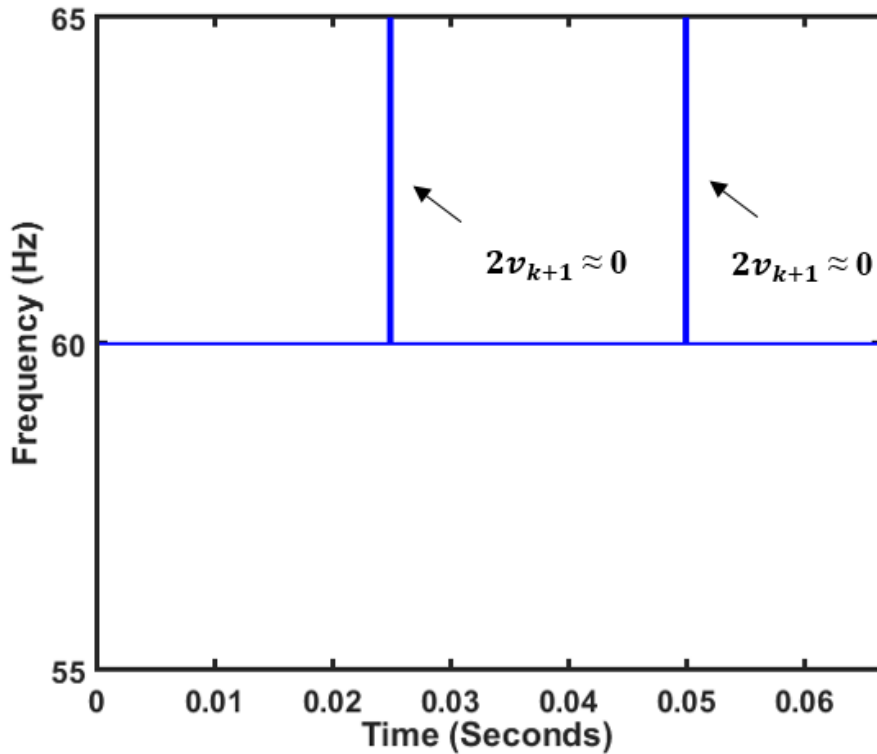
Figure 13: Frequency estimation using the adjustment points method

Figure 13 shows the measured frequency value of a 60 Hz sinusoid, using the

adjustment points method. To ensure these spikes in frequency estimation don't occur,

Equation (14) should not be computed when $2v_{k+1}$ is close to zero. To avoid this,

conditions could be set to only estimate frequency when [21]:

$$T \geq 2v_{k+1} \leq -T \tag{15}$$

Where: T = the established threshold to avoid zero (e.g. 0.001)

By applying the condition in Equation (15), the updated frequency estimation is

shown below:
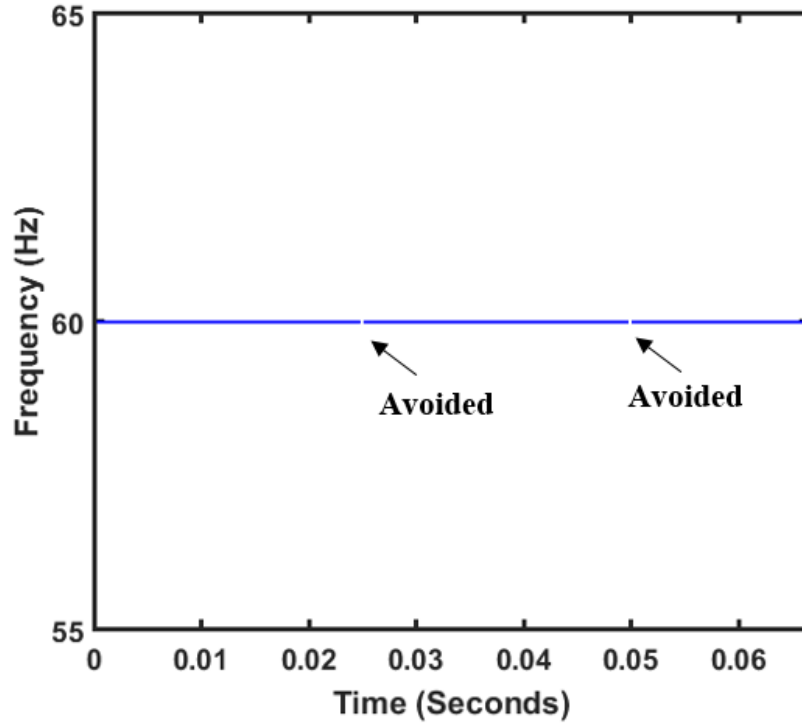
Figure 14: Avoiding frequency estimation when $2v_{k+1}$ is close to zero

Notice the frequency estimation is cleaner by applying the condition in Equation (15). This allows the frequency value to be updated with each new sample obtained, if the samples satisfy the specified condition. There is an additional way to remove the effects of $2v_{k+1}$ being zero and it allows the condition in Equation (15) to be detached as well. In [21], the following ratio is established:

$$\frac{v_k + v_{k+2}}{2v_{k+1}} = \frac{v_{k+3} + v_{k+5}}{2v_{k+4}} = \frac{v_{k+6} + v_{k+8}}{2v_{k+7}} = \ldots = \frac{|v_k + v_{k+2}| + |v_{k+3} + v_{k+5}| + |v_{k+6} + v_{k+8}| + \ldots}{|2v_{k+1}| + |2v_{k+4}| + |2v_{k+7}| + \ldots} \quad (16)$$

The relationship in Equation (16) is developed to modify Equation (14) and , the result is defined in Equation (17) as follows [21]:

$$f = \frac{1}{2\pi t_s} \cos^{-1}\left(\frac{\sum_{k=1}^{n} |v_k + v_{k+2}|}{\sum_{k=1}^{n} |2v_{k+1}|}\right) \quad (17)$$

The response of Equation (17) is graphed below, with a 60Hz signal applied.
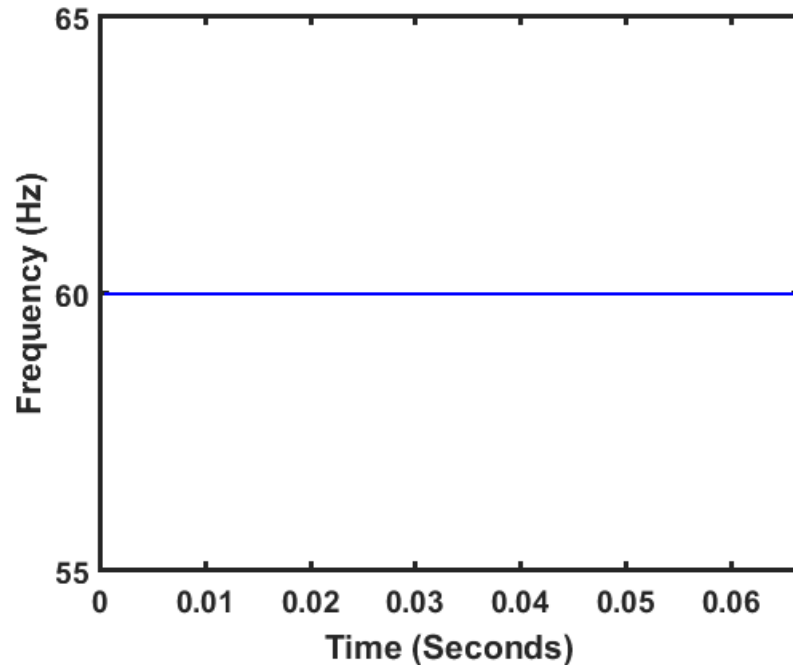
Figure 15: Avoiding when $2v_{k+1}$ is close to zero by using summation windows

Notice the response in Figure 15 does not have any un-avoided computation like that of Figure 14; therefore, the frequency estimation can be updated with each new sample obtained. By including more samples into the frequency estimation of Equation (17), the response is no longer affected by zero within the denominator. In addition, the frequency estimation becomes stable by utilizing more samples from the signal [21].

Figures 13, 14, and 15 show the frequency estimate for a sinusoid signal that is constant in frequency, harmonic free, and noise free. However, power system signals can often include waveform distortion. The figure below illustrates the effect that harmonics have on the adjustment point method.
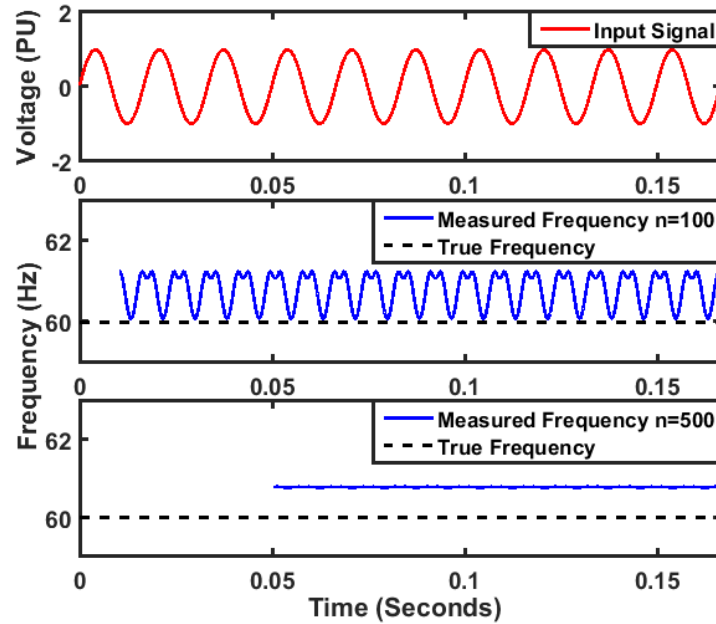
Figure 16: Adjustment point method with harmonic content

The input signal in Figure 16 includes a 60 Hz signal with 1 percent 3rd harmonic. The two bottom graphs demonstrate the differences in frequency estimation by increasing the summation window, denoted by n. By increasing the window, the estimation becomes cleaner; however, both graphs show that the frequency estimation includes large errors with minimal harmonic content. The effects of noise on the method is demonstrated below:
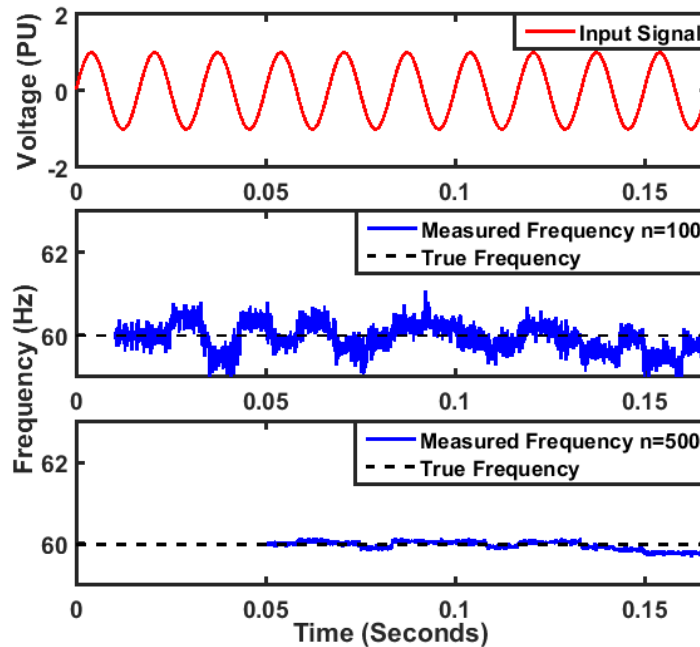
Figure 17: Adjustment point method with noise included

In Figure 17, the input voltage signal includes noise with a signal-to-noise ratio

(SNR) of 60 dB. A typical SNR of a voltage signal in the power system is 50 dB - 70 dB

[24]. When increasing the summation window, the effects of noise was improved. To

further improve signal accuracy pre-filtering is used. Pre-filtering increases the accuracy

of the adjustment point method [21]. This method requires more pre-filtering than that

of the zero-crossing. The zero-crossing is only affected by harmonics if the harmonic

content imposes multiple zero-crossings, where the adjustment point method is very

sensitive to noise and harmonics. This method requires pre-filtering to ensure the noise

and harmonic content is removed or attenuated.

2.3.1.3 Discrete Fourier Transform

A phasor is a representation of a sinusoidal signal for a given time with respect to

a time reference. Phasors include both magnitude and phase angle quantities. Using the

equation to describe the sinusoidal signal, the following equation can be used to describe

a sinusoidal signal as its corresponding phasor [25]:

$$V = \frac{V_m}{\sqrt{2}} e^{j\Theta}$$
(18)

Where: V = phasor representation of sinusoidal signal

V_m = amplitude of the sinusoidal signal (volts)

e = base of natural logarithm

Θ = phase angle (radians)

$j = \sqrt{-1}$

It has been identified in [18, 26] that frequency can be estimated using the rate-of-

change-of phase angle (Θ). This can be represented as the following:

$$f = \frac{1}{2\pi} \cdot \frac{d\Theta}{dt}$$
(19)

Where: f = frequency (radians/sec)

π = mathematical constant

t = time (seconds)

Θ = phase angle (radians)

Defining frequency as the rate-of-change-of phase angle is implemented widely

throughout PMUs [18]. Before Equation (19) can be used to determine the frequency,

understanding how the phasor is estimated is essential. One way phasors can be

estimated is using the discrete Fourier transform (DFT) [18]. Equation (20) illustrates the

exponential form a of DFT equation [27]:

$$X(m) = \sum_{n=0}^{N-1} x(n) e^{-j2\pi nm/N}$$
(20)

Where: $x(n)$ = discrete sample values

$$X(m) = \text{DFT output component}$$

$$n = \text{time-domain index of samples}$$

$$N = \text{number of sequence samples}$$

$$m = \text{frequency-domain index of the DFT}$$

Two additional equations can be utilized to further expand Equation (20) into a more recognizable form. The first equation defines the phase angle for the mth DFT output component as:

$$\theta = 2\pi m/N \tag{21}$$

The second equation needed refers to Euler's relationship [27]:

$$e^{-jn\theta} = cos(n\theta) - jsin(n\theta) \tag{22}$$

Using Equations (21) and (22), the rectangular form of Equation (20) can be displayed as:

$$X(m) = \sum_{n=0}^{N-1} x(n)[\cos(n\theta) - jsin(n\theta)] \tag{23}$$

The rectangular form in Equation (23) allows the real and imaginary components to be evaluated separately. To understand how Equation (23) yields an estimate of a phasors magnitude and angle, the figure below is used for illustration:
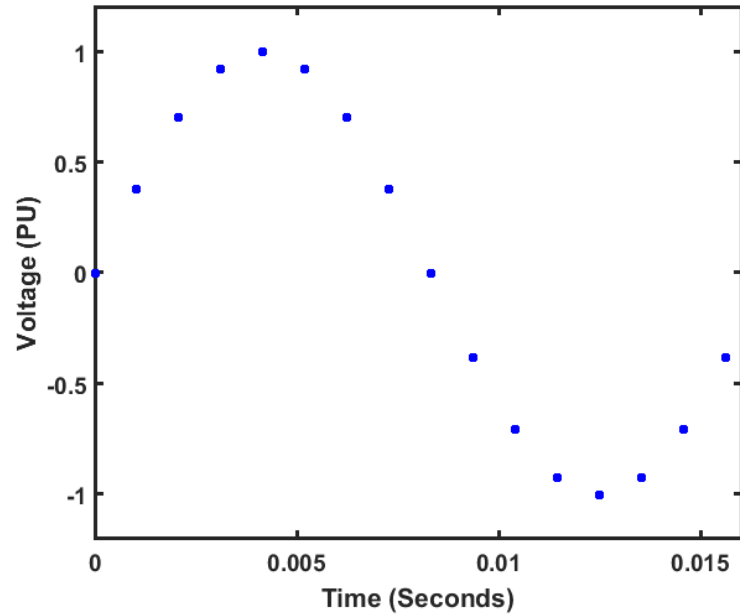
Figure 18: Sampled sinusoidal signal

Figure 18 contains a fundamental frequency of 60 Hz, with a sampling rate that corresponds to 16 samples/cycle. This means that in one cycle there are exactly 16 samples that are equally spaced in time. The interesting part of Equation (23) is that the frequency-domain index, m, correlates to the direct integer multiple of samples/cycle. This is shown in the following formula [27]:

$$Frequency(m) = \frac{mf_s}{N} \tag{24}$$

Where: f_s = sampling frequency

N = number of sequence samples

In this case the sampling frequency (f_s) is 960 Hz and the number of sequence samples (N) is 16. This translates to a frequency of 60 Hz for a frequency-domain index of m=1. So, if $m = 1$ this will extract the phasor information that links to the 60 Hz frequency component. If m = 2, this will extract the 2nd harmonic (120 Hz) phasor information of the signal, if m=3 this will extract the 3rd harmonic (180 Hz) phasor

information of the signal etc. This relationship allows for a filtered phasor estimation for

the power system frequency (if the exact number of samples per power system cycle are

known). For this reason, when evaluating the fundamental frequency component, the m-

value can be set as one in Equation (21). Furthermore, Equation (21) can now be

represented as:

$$\theta = 2\pi/N \tag{25}$$

An additional magnitude modification is required in Equation (23) to adjust the

phasor to the proper value. When evaluating the DFT in Equation (23) on the sampled

values in Figure 18, the resulting magnitude is eight. It is obvious from the graph that the

maximum value obtained is one, yet the DFT yields a magnitude of eight. To scale the

magnitude to the appropriate level, the following formula is utilized [27]:

$$A_o = \frac{2M_r}{N} \tag{26}$$

Where: A_o = peak amplitude of sinewave

M_r = DFT magnitude of sinewave

N = number of sequence samples

Equation (26) is still incomplete, since the value obtained will yield the peak

amplitude of the particular sinewave of interest [27]. To modify this one step further, the

peak amplitude of the sinewave (A_o) must be divided by the square root of two to obtain

the corresponding magnitude of the evaluated sinewave. Using this concept with

Equation (26), Equation (23) will be slightly changed as follows [5, 26]:

$$X(m) = \frac{\sqrt{2}}{N} \sum_{n=0}^{N-1} x(n)[\cos(n\theta) - j\sin(n\theta)] \tag{27}$$

Equation (27) yields a magnitude value of ≈ 0.7071 when m =1 for the samples in

Figure 18, as expected. The corresponding phasor angle (θ) is utilized when determining

frequency and/or frequency deviations [26]. It may be preferred to update the estimated

phasor value with each new sample obtained; there is a well-established method for

updating phase angle measurements using the DFT based method. In [5], the

fundamental frequency is determined using recursive updates of the phase angle.

The recursive method undergoes a slight modification when compared to

Equation (27). The recursive form starts by multiplying both each side of Equation (27)

by $e^{-j\theta}$, as seen below [5]:

$$X(m)(e^{-j\theta}) = \frac{\sqrt{2}}{N}\sum_{n=0}^{N-1} x(n)e^{-j\theta n}(e^{-j\theta}) \tag{28}$$

Equation (28) can be rearranged using the exponential components and adjusted

using the concept in Equation (25) as follows [5]:

$$\hat{X}^{N-1} = X^{N-1}e^{-j\theta} = \frac{\sqrt{2}}{N}\sum_{n=0}^{N-1} x(n)e^{-j\theta(n+1)} \tag{29}$$

The modification in Equation (29) is based on what occurs when the data window

shifts. Once the data window shifts one sample, the oldest sample is lost and the newest

sample is added. A more intuitive form of Equation (29) is displayed below [5]:

$$\hat{X}^{N} = \hat{X}^{N-1} + \frac{\sqrt{2}}{N}(x_N - x_0)e^{-j(0)\theta} \tag{30}$$

Equation (30) is useful to save computational resources [5]. To determine the

estimate for phasor N, two things need to occur to phasor estimate N-1: one is to add the

additional effects of sample x_n and second is to remove the influence of the last data

sample x_0 (which is shifted out of the new data window). In [5], a convenient way to

simplify this as a continuous process is to include 'r' as the recursive phasor estimate

number. Equation (30) is adjusted to include the variable 'r'.

$$\hat{X}^{N+r} = \hat{X}^{N+r-1} + \frac{\sqrt{2}}{N}(x_{N+r} - x_r)e^{-jr\theta} \tag{31}$$

When performing Equation (30) on constant signal and sampled at a fixed number of samples per power system cycle, the resulting phasor diagram is as seen below:
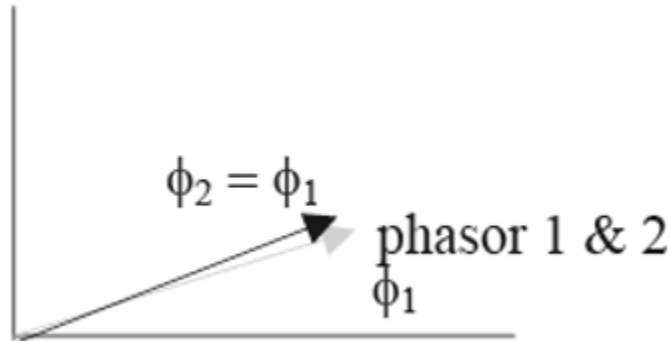
Figure 19: Recursive phasor update [5]

In Figure 19, the phasors are fixed in angle for a signal that is constant in frequency. In Figure 18, there is exactly 16 samples in one cycle of a 60 Hz signal, resulting in a sampling frequency of 960 Hz. As the sampled signal progresses in time the phase angle will always be maintained if the frequency does not change. Figure 18 is a representation of the following signal:

$$X(t)_{per\ unit} = \sin(120\pi t) \tag{32}$$

Table 4 below demonstrates 25 samples of the signal produced in Equation (32) and the corresponding phase angle measurement determined by Equation (30).

Table 4: DFT recursive based method for 60 Hz reference signal

Sample Number	Sample $X(t)$	Phase Angle (deg.)
1	0.0000	-
2	0.3827	-
3	0.7071	-
4	0.9239	-
5	1.0000	-
6	0.9239	-
7	0.7071	-

8	0.3827	-
9	0.0000	-
10	-0.3827	-
11	-0.7071	-
12	-0.9239	-
13	-1.0000	-
14	-0.9239	-
15	-0.7071	-
16	-0.3827	-
17	0.0000	90.0000
18	0.3827	90.0000
19	0.7071	90.0000
20	0.9239	90.0000
21	1.0000	90.0000
22	0.9239	90.0000
23	0.7071	90.0000
24	0.3827	90.0000
25	0.0000	90.0000

Notice in Table 4 that the calculated phase angle does not change. Now let's

consider the signal varying in frequency while sampling at a fixed 960 Hz rate.

$$X(t)_{per\ unit} = \sin(120\pi t + 1\pi t^2) \tag{33}$$

The above equation is a mathematical representation of a ramp in frequency. The

frequency starts at 60 Hz at time = 0 and increases the frequency linearly at a 1 Hz/s rate.

Table 5: DFT recursive based method for 1 Hz/s frequency ramp

Sample Number	Sample $X(t)$	Phase Angle (deg.)
1	0.0000	-
2	0.3827	-
3	0.7071	-
4	0.9239	-
5	1.0000	-
6	0.9238	-
7	0.7070	-

8	0.3825	-
9	0.0002	-
10	0.3829	-
11	0.7073	-
12	0.9240	-
13	1.0000	-
14	0.9237	-
15	0.7066	-
16	0.3820	-
17	0.0009	89.9795
18	0.3836	89.9785
19	0.7079	89.9747
20	0.9243	89.9780
21	1.0000	89.9780
22	0.9233	89.9792
23	0.7059	89.9720
24	0.3810	89.9813
25	0.0020	89.9796

Table 5 above shows the calculated phase angle fluctuating. This is an indication that the sample rate does not contain an integer number of samples/cycle. Table 4 describes a 60 Hz waveform with exactly 16 samples/cycle sampling rate; therefore, the calculated angle did not deviate from one sample to the next.

The change in phase angle is directly related to the change in frequency [26]. In [26], the relationship between frequency deviation and phase angle change is described as:

$$\theta_r = \theta_{r-1} + \frac{\Delta f}{60} \cdot \frac{2\pi}{N} \qquad (34)$$

Where: θ_r = recursive phase angle update

Δf = frequency deviation

The θ_{r-1} refers to the phase angle value that occurs just before θ_r. The 60 in this equation applies to a nominal system frequency of 60 Hz. The frequency deviation can be solved for as follows [26]:

$$\Delta f = \frac{(\theta_r - \theta_{r-1})60N}{2\pi} \qquad (35)$$

This equation is more formally represented as the derivative of the phase angles [26].

$$\frac{d\theta}{dt} = \Delta f 2\pi \qquad (36)$$

Using Equations (35) and (36) the frequency measurement can be expressed as [26]:

$$f = 60 + \Delta f \qquad (37)$$

The graph below illustrates the measurement response of the DFT based method:
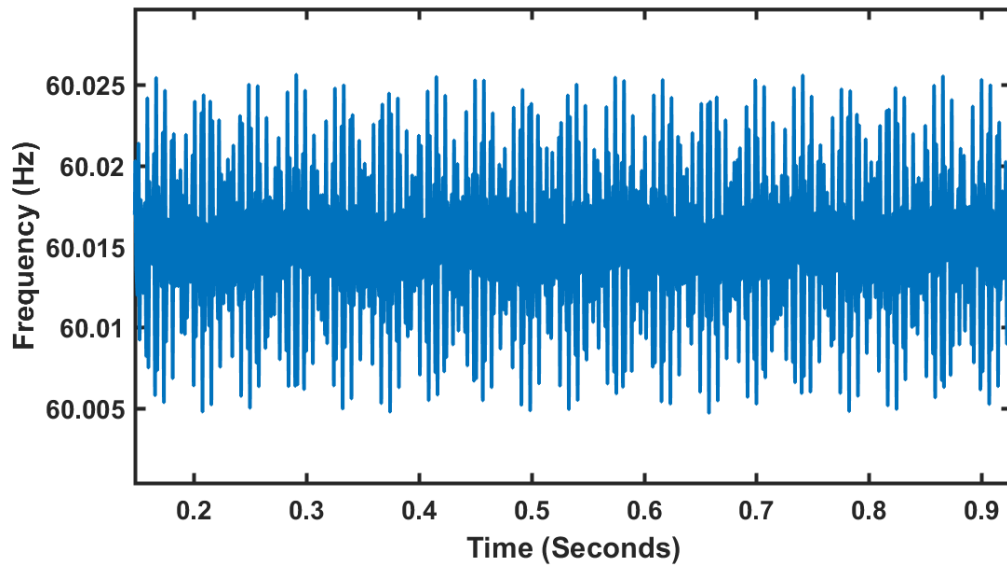
Figure 20: Recursive based DFT method measurement response

The input signal for the above measurements included a fundamental frequency of 60.010 Hz. The input signal was sampled at a fixed 1020 Hz. This is equivalent to a 17 samples/cycle for a fundamental frequency of 60 Hz. Notice, the measurement fluctuates

through time. Taking the derivative can amplify noise within measurements. The maximum error measured in the graph is approximately 15 mHz. However, the fluctuation can be reduced, thus improving the accuracy by filtering the measured frequency. The filtered response can be seen below:
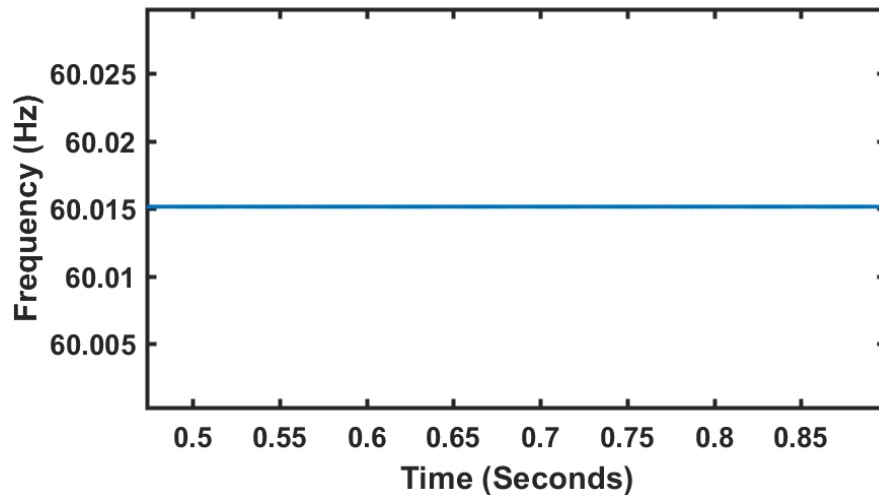
Figure 21: Recursive based DFT method filtered measurement response

The scale on the y-axis remains the same as for Figure 20. The filtering attenuated the measurement fluctuation and improved the overall accuracy of this method. The maximum error seen in Figure 21 is now 5 mHz.

The recursive based DFT is a very effective way to estimate system frequency. This could be implemented in hardware using a variable sampling clock or a fixed sampling clock. If this were implemented within a variable sampling clock, there would be a feedback loop included. To maintain a fixed integer samples/cycle the ADC must adjust the time between samples. To adjust the time between samples, the frequency estimation method must feedback to the sampling clock. This is referred to as frequency tracking. This is shown is the figure below:
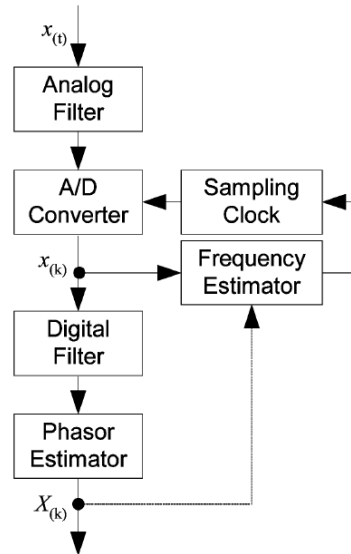
Figure 22: Frequency tracking [5]

Figure 22 illustrates that frequency is computed using the samples obtained from

the ADC then the Δf is fed back to the sampling clock to properly adjust the time

between samples. If no Δf is measured at that instance, the sampling clock will maintain

its current sampling rate.

2.3.2 Time-stamping Frequency Measurements

Synchrophasors consist of phasors, frequency, and rate-of-change-frequency

(ROCOF) measurements that are reported at specific time instances with respect to an

absolute time source [6, 7]. The measurements are tagged with the true time of

occurrence, which in most cases is the center of the computation window. The industry

standard defining the sychrophasor measurements in power systems is the IEEE std.

C37.118.1a-2014 [7]. Per that standard, synchrophasor measurements require time

compensation when time stamping the measurement, which will allow for direct

comparison of readings at any instance of time across the power system between any type

of PMUs. There are several aspects of frequency measurements which will create an

inherent delay in the time when frequency was calculated versus the instance in time

when the corresponding value occurred (e.g. due to anti-aliasing filter, digital filtering, and window size). When sampling a continuous time signal an analog low pass filter (LPF) is required to prevent aliasing [5, 22]. In addition, any digital filtering and window selection size could add additional delays to the measured time of frequency. To apply synchrophasors these inherent delays must be compensated for to reflect the true time of occurrence. Assuming the LPF and digital filtering delay is linear across all frequencies, this can be compensated for by applying the proper correction time. The graph below illustrates this concept:
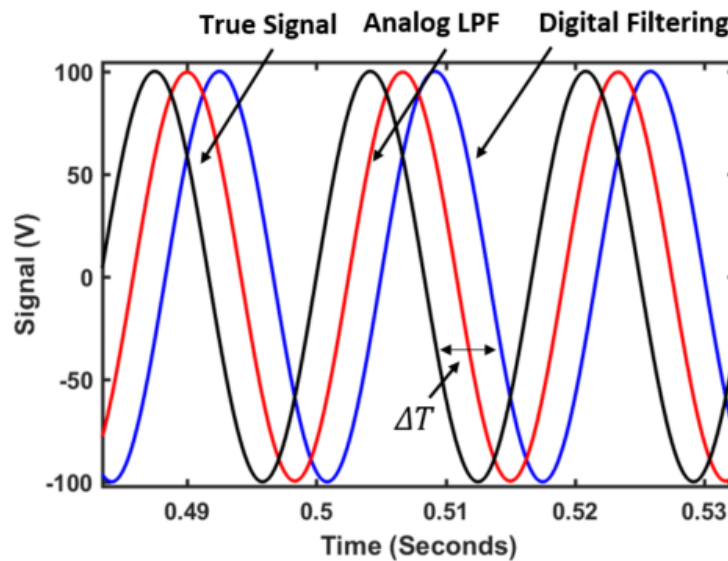
Figure 23: Time compensating filter delay

Figure 23 displays two inherent delays from the measured signal. The analog LPF lags the true signal, and the digital filtered signal results in an additional lag. Thus, requiring a time compensation of ΔT. The implemented frequency measurement method would be performed on the digital filtered signal. In some methods such as presented in [17], digital pre-filtering is not necessary, so the frequency calculation would begin on the digital samples directly obtained from the ADC.

There are additional delays that are inherent to the measurement methods. The implemented window size for the frequency method will create a delay as well. Consider a frequency measurement performed on a four cycle window and the time tagging in the center of the window [28]. This would provide the actual time of occurrence; however, a two-cycle time compensation would be required when applying as a synchrophasor measurement. Additionally, any post filtering would impose a delay as well which would require compensation.
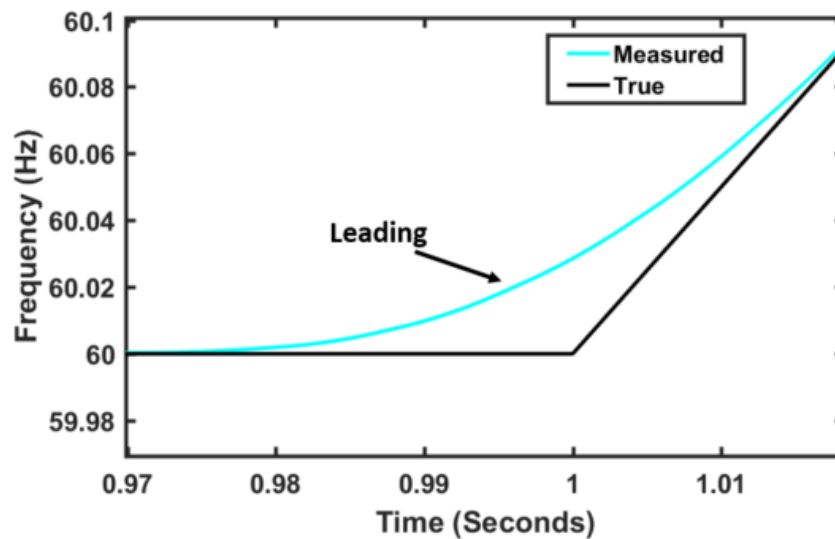
Figure 24: Leading frequency measurement

Figure 24 displays the fundamental frequency component ramping at a linear rate one second into the plot. The measured response is leading the true response as this transition occurs. This is misleading in that the frequency measurement is not predicting the frequency deviation, the leading measurement is strictly an artifact of time tagging the center of the data window for the frequency measurement. When time tagging the center of the window, the frequency measurement will contain both past and, what will appear as, future data. Approximately 20 ms into the frequency variation the measurement

yields very little error, on the order of $\pm$ 2 mHz. This shows that appropriate time compensation has been applied.

CHAPTER 3: METHODOLOGY

3.1 New Frequency Estimation Method

This section proposes an alternative method to estimate power system frequency. The goal of the proposed method is to allow for fast and accurate measurements throughout the various events encountered on the system. In addition to updating the frequency measurement with each new sample obtained. The method includes several benefits that could be utilized to further the development and understanding of digital signal processing (DSP) for frequency algorithms. The method allows for the frequency value to be updated with each new sample obtained from the PMU device. This opens the possibility of increasing the frequency reporting rate where other methods may be limited by. The updated reported frequency value for the new method is only limited by processing capabilities of the microprocessor device and the implemented sampling frequency. The following sub-sections discuss the operating principles of the new method, along with the key stages involved.

3.1.1 Pre-Filtering Stage

Many frequency estimation methods include a pre-filtering stage that will assist in the attenuation of noise on the measured digital samples. Noise will impact each method differently depending upon the intricacies of the technique in question. The pre-filtering stage for this method is classified as a finite impulse response (FIR) [27]. An FIR filter is impactful in digital signal processing (DSP) to remove, attenuate, and/or extract a

frequency of interest. In addition, this type was chosen to allow for a linear group delay.

A linear group delay can be conveniently compensated when synchrophasor

measurements are applied. The implemented FIR filter for this analysis is a three-stage

average. The multiple stages allow for further noise attenuation. Each of the three stages

contains 40 samples of the measured signal. The figure below illustrates this concept.

$$\frac{V_{k-39} + V_{k-38} + V_{k-37} \ldots V_{k-3} + V_{k-2} + V_k}{40}$$

$$\frac{V_{k-39} + V_{k-38} + V_{k-37} \ldots V_{k-3} + V_{k-2} + V_k}{40}$$

$$\frac{V_{k-39} + V_{k-38} + V_{k-37} \ldots V_{k-3} + V_{k-2} + V_k}{40}$$
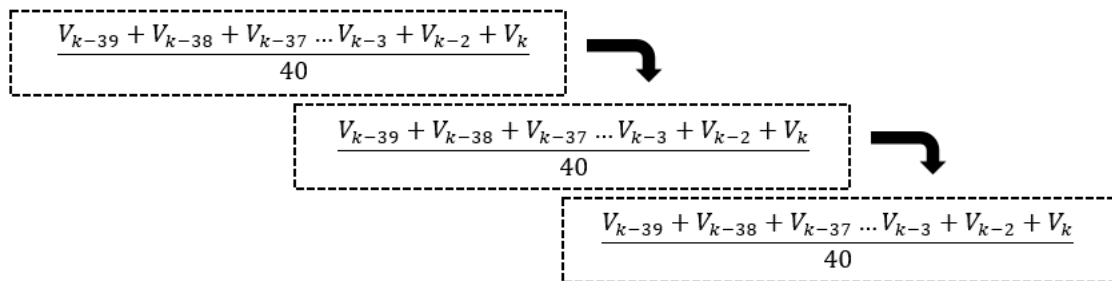
Figure 25: Three-stage average FIR filter

Figure 25 displays the three-stage filter process. The chosen filter type was a

simple, yet effective way to attenuate noise across the frequency spectrum. Minimal

window lengths are desired to achieve shorter group delays. The window length and

filter type allowed the proposed method to achieve accuracy while maintaining minimal

delay. Each stage consists of 40 data samples; the average of the 40 data samples will be

placed within stage two. Stage two works in the same fashion, 40 data samples are

averaged and passed to the last pre-filtering stage. After the final average stage, the

filtered samples are used for the determination of system frequency. Ideally, no pre-

filtering would be used on any method [17]. However, the proposed algorithm, like most,

requires pre-filtering to improve the accuracy of the frequency estimator. The benefits of

the pre-filtering stage are illustrated in the following figure.
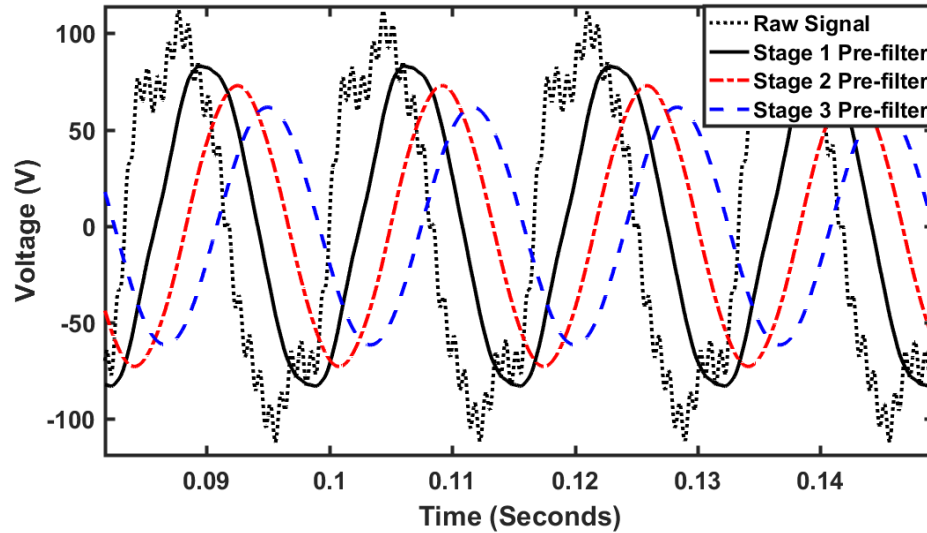
Figure 26: Three-stage average FIR filtered signal

Figure 26 displays the effects of each stage of the three-stage filtering process, along with the raw measured signal. Notice the raw measured signal is distorted with several harmonics. The first pre-filtering stage attenuates most of the additive harmonics; however, the waveform remains distorted. To further attenuate the noise superimposed on the raw signal, there are two additional filtering stages. The average filter not only attenuates the harmonics, but attenuates the fundamental frequency component. This would not work well for phasor estimators, since the magnitude is attenuated; however, this does not impose any negative effect for the proposed frequency algorithm.

Also, as explained earlier, the filtering will impose an inherent measurement delay (lag) when compared to the actual signal. This is obvious when comparing the time stamps for each of the filtered stages with respect to the raw signal in Figure 26. With each additional filtering stage, there is more lag in the measured signal. Fortunately, this lag is fixed in the number of samples and can easily be compensated for when applying synchrophasors. The third stage average filter is the input to the proposed frequency estimation method. The method is discussed throughout the next section.

3.1.2 BC Frequency Estimation Method

The goal of the BC method was to provide an accurate way to update the value of frequency at the same rate as the sampling frequency for the input signal. In addition to providing an alternative definition for determining the frequency of a signal. To achieve this, the method could not rely on any specific event such as a zero crossing.

3.1.2.1 Superimposed Angle Calculation

The approach of the BC method is to transform the sinusoidal power system signal, voltage and/or current, into another form which will allow for frequency to be computed at the update rate of the sampling frequency. An essential of any frequency estimation method is the time between each sample or inversely, the sampling frequency. In most methods, the sampling frequency rate will influence the accuracy of the algorithm. For the simulations of this method, a sampling frequency of 8 kHz is used for the implementation.

The BC method starts with assigning an angle to each sample, as seen in Equation (38), based on two measured samples that are separated by an integer number of samples.

$$B(k) = \tan^{-1}(\frac{lookback}{V_k - V_{k-lookback}}) \qquad (38)$$

Where: $B(k)$ = established angle for sample k

                 V_k = most recent value at sample k

                 $lookback$ = an integer number of samples prior to sample k

This concept shown in Equation (38), is illustrated in the figure below:
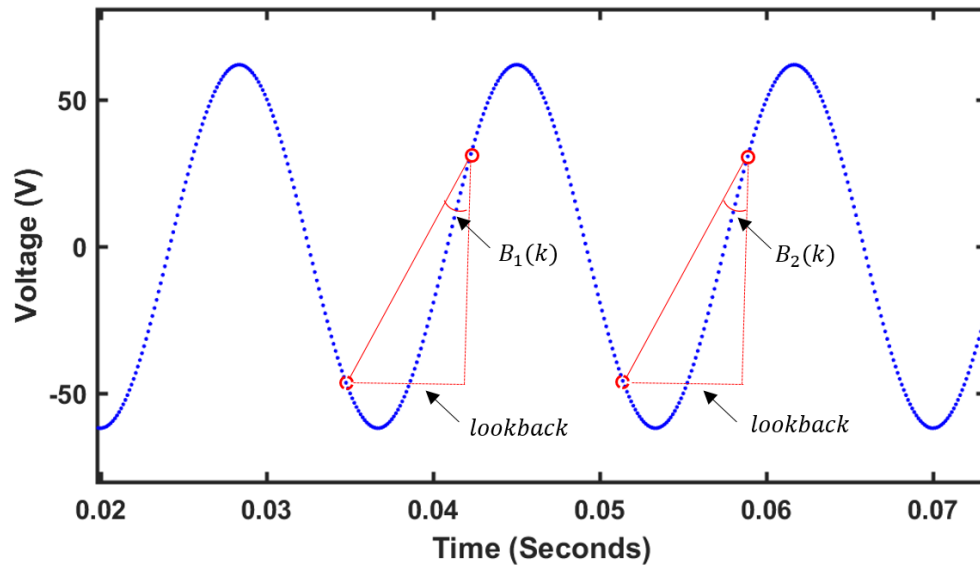
Figure 27: Superimposed angle calculation

Figure 27 shows a sampled sinusoidal waveform. Each sample obtained from the signal includes an x- and y-coordinate. The x-coordinate is simply the sample number or timestamp obtained from the measurement system. The timestamp and sample number can be used interchangeably when the implementation includes a fixed sampling frequency. For instance, in the figure the lookback value is fixed throughout and may be user selected to any value. If the lookback value is 30 samples, then the delta-t for the lookback value is simply the lookback value multiplied by the inverse of the sampling frequency. This explains that the $B(k)$ function establishes a new angle using two samples with a fixed separation in time and/or sample number. The y-coordinate in the figure is the sampled voltage value. Using the relationship of the sampled x- and y-values, a superimposed angle can be established using the Pythagorean theorem. This is performed with each new sample obtained from the algorithm.

This method ultimately determines the system frequency by evaluating when $B_1(k)$ equals $B_2(k)$ and computing the sample difference between the two angles. The

angle difference will yield the numbers of samples/cycle, which can easily be converted

to frequency. One thing to consider for the evaluation is $B_1(k)$ will only equal $B_2(k)$

when the sampling frequency is an integer multiple of the system frequency. To further

illustrate the idea, Figure 28 shows a voltage signal, with a fundamental frequency of 60

Hz, that was sampled at a rate of 960 Hz.
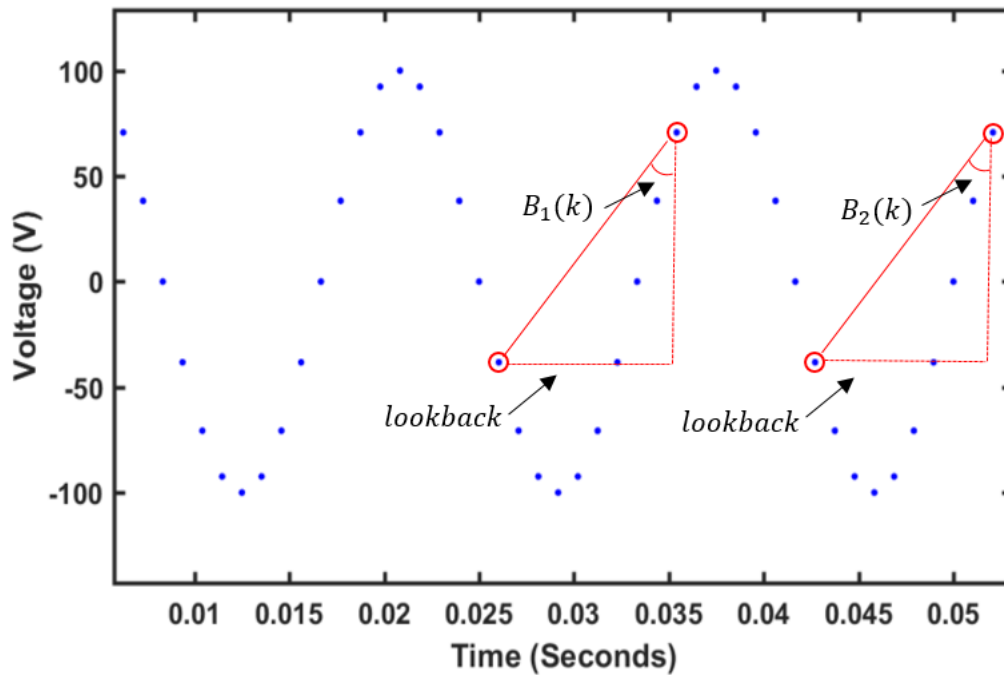
Figure 28: Superimposed angle calculation with 960 Hz sampling

Figure 28 illustrates a voltage that was sampled at 960 Hz for illustration

purposes; this is not the suggested sampling frequency for the proposed method. The

selected *lookback* value was nine samples. Using the measured samples in Figure 28

and the angle calculation in Equation (38), the following values were obtained.

Table 6: Superimposed angle calculation

Sample Number, k	Sample Value, V_k	Angle, $B(k)$
1	-38.268	-
2	-70.71	-
3	-92.39	-
4	-100	-

5	-92.39	-
6	-70.71	-
7	-38.27	-
8	0	-
9	38.27	-
10	70.71	4.721
11	92.39	3.158
12	100	2.678
13	92.39	2.678
14	70.71	3.158
15	38.27	4.721
16	0	13.234
17	-38.27	-13.234
18	-70.71	-4.721
19	-92.39	-3.158
20	-100	-2.678
21	-92.9	-2.678
22	-70.71	-3.158
23	-38.27	-4.721
24	0	-13.234
25	38.27	13.234
26	70.711	4.721

Table 6 shows the established angle calculations, $B(k)$, for the measured samples in Figure 28. Notice, that a new angle is assigned to each obtained sample and the angle at sample 26 equals the angle at sample 10. This yields that a full cycle occurred between samples 26 and 10. The frequency, or time occurrence of a cycle, can be computed using the samples and the known sampling frequency. This is shown below:

$$frequency = \frac{f_s}{k_{B2} - k_{B1}} \qquad (39)$$

Where: f_s= sampling frequency

k_{B1}= assigned sample for $B_1()$

k_{B2}= assigned sample for $B_2(k)$

$frequency$ = calculated system frequency

For the values in Table 6, the calculated system frequency is 60 Hz. There are two obvious issues when evaluating the established angles in Table 6. First, the sampling frequency does not have to be an exact integer multiple of the system frequency; therefore, it is unlikely for any two established angle calculations to be identical. Second, when applying the angle calculation, Equation (38), on a sinusoidal waveform, the established angle will occur more than just once before a full cycle occurs. Notice, samples 10 and 26 were used to compute frequency; however, the established angle, 4.721 degrees, also occurs on sample 15. Both issues are addressed moving forward.

3.1.2.2 Solving for Angle Re-Occurrence by Interpolating

As mentioned, the sampling frequency is unlikely to be an exact integer multiple of the system frequency; therefore, to ensure the accuracy of the method, interpolating is required. When knowing two sets of x- and y-coordinate values, a value that falls within the two sets can be interpolated when one coordinate is specified. The x-coordinate, in this case, is the measured sample number and the y-coordinate is the sample voltage value. The figure below displays this concept.
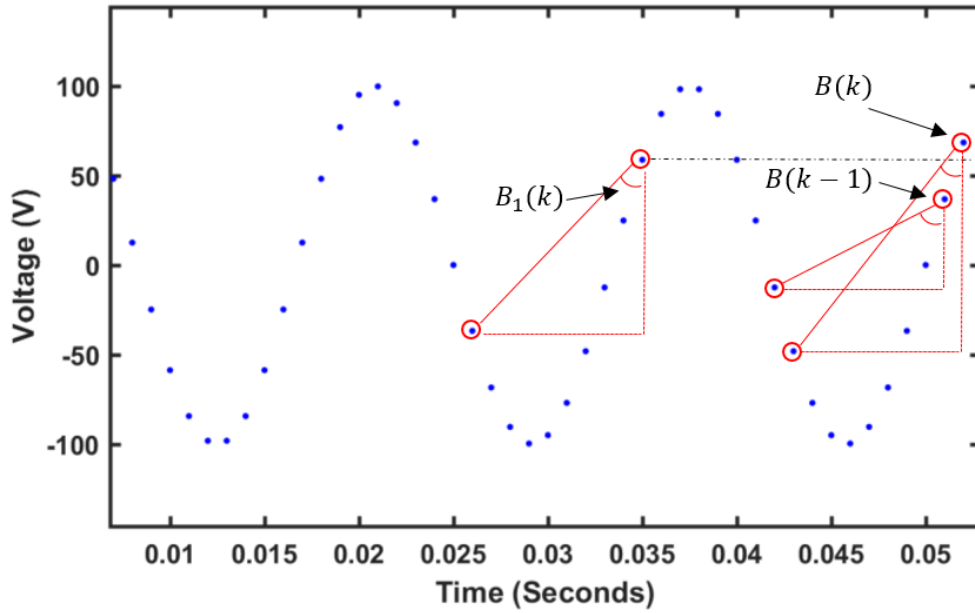
Figure 29: Superimposed angle calculation with 1000 Hz sampling

Figure 29 illustrates that there is not a fixed number of integer samples per

sinusoidal cycle. The signal in question contains a fundamental frequency of 60 Hz and

the sampling frequency is 1000 Hz. This yields that there is ≈ 16.667 samples in one

cycle. The calculated angle, $B_2(k)$, falls between calculated angles $B(k-1)$ and $B(k)$.

To determine the sample number where $B_2(k)$ truly occurs Equations (40) and (41) are

used.

$$B(k) - B_1(k) = \Theta_k \tag{40}$$

Where: $B(k)$ = most recent established angle

$B_1(k)$ = established angle one cycle prior to $B_2(k)$

Θ_k = angle difference of $B(k)$ and $B_1(k)$

$$B(k-1) - B_1(k) = \Theta_{k-1} \tag{41}$$

Where: Θ_{k-1} = angle difference of $B(k-1)$ and $B_1(k)$

A full cycle occurs exactly when $B_1(k)$ equals $B_2(k)$, this is the same as when the

difference of $B_2(k)$ and $B_1(k)$ is zero. Knowing this, using the calculated values Θ_k and

Θ_{k-1}, along with the sample number at which they are assigned, an interpolated value

can be achieved. The table below includes the values that pertain to Figure 29 for the

interpolation calculation.

Table 7: Values used in interpolation calculation

	Sample Number	Value
$B_1(k)$	35	3.791
$B(k-1)$	51	5.379
$B(k)$	52	3.369
Θ_{k-1}	51	1.588
Θ_k	52	-0.422

Table 7 yields the values necessary to interpolate the sample at which $B_2(k)$

occurs. The value for Θ_k is assigned the same sample number as $B(k)$. Likewise, the

value for Θ_{k-1} is assigned the sample number of $B(k-1)$. The interpolation will solve

for the sample number when a value of zero occurs, this takes into consideration that the

difference of $B_2(k)$ and $B_1(k)$ is zero. The simplest form of interpolation is linear

interpolation. It only requires two sets of x- and y- coordinates, along with a specified

point that falls within the two coordinate sets. The specified point for this calculation

will always be zero. Two forms of interpolation are used for the proposed frequency

method, linear and quadratic. The implemented quadratic interpolation uses three known

sets of x- and y- coordinates, where the linear interpolation method only uses two sets.

The quadratic interpolation method is first executed and if the found roots are not found

within the specified sample numbers, in the case of Table 7: 51 and 52, then linear

interpolation method is used as an alternative.

3.1.2.3 Frequency Reporting Calculation and Validation

As noted previously, there are instances when $B_1(k)$ could equal $B_2(k)$ before the

full sinusoidal period occurs. Rather than developing sophisticated detection logic to

ensure that a false value of frequency is not reported, when $B_1(k)$ equals $B_2(k)$ prior to a

full cycle, the known occurrence is utilized to identify when a true power system cycle

has occurred. The angle calculation for this method that has been discussed throughout is

useful when determining when a signal replicates. To illustrate this, the superimposed

angle calculation for this method is graphed below:
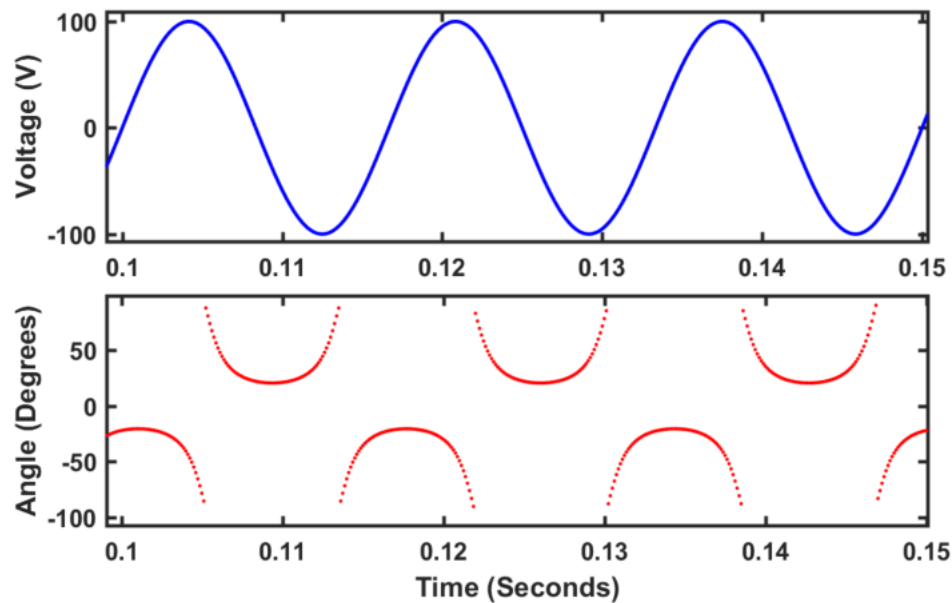
Figure 30: Measured waveform and angle calculation

Figure 30 displays the measured voltage signal on top and the graphed angle

calculation for the signal on bottom. Notice, the signal is simply transformed from a

sinusoidal waveform to another form that replicates at the same frequency of the

measured signal. As stated before, any given calculated angle occurs more than once in a

full cycle for a sinusoidal signal. To eliminate inaccurate reporting, the algorithm counts

to four. To further explain, the angle calculation is graphed below illustrating this

concept.
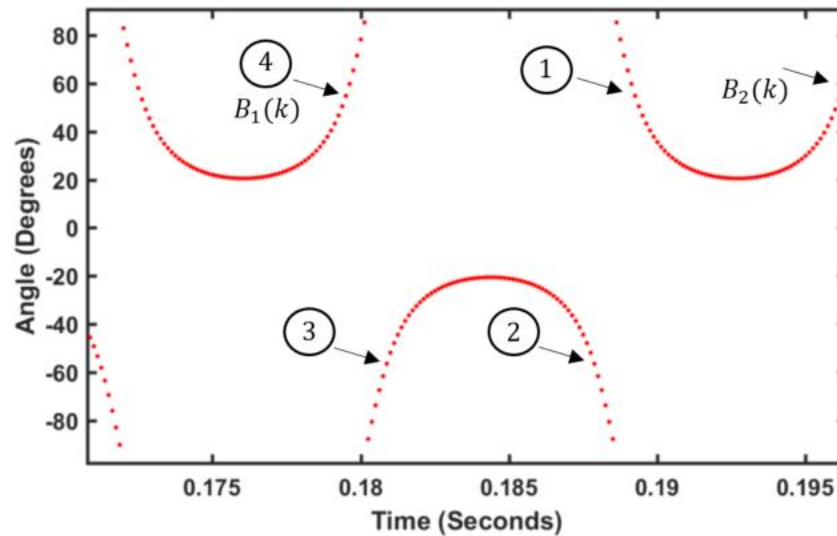
Figure 31: Angle calculation using four-count

If an absolute value was taken on all calculated angles, $B(k)$, the angle would

occur four times for any given cycle. The absolute value is not used here, but a similar

concept of the angle reoccurring four times can be seen in Figure 31. Recall, when

interpolating the sample number where $B_2(k)$ occurred, the difference of the most recent

angle and $B_1(k)$ was made. The difference is not only used throughout for interpolation,

but also to count the number of sign change transitions. Figure 31 shows that $B_1(k)$ will

equal $B_2(k)$ with four sign change transitions. To explain further, consider the data

window in which the calculated angles are stored.

A moving data window is utilized for the BC method to store only the necessary

number of calculated angle values in memory. The data window is of a fixed length; the

length is selected based on the minimum frequency of interest. The guideline for the

established window length is listed below:

$$W_l = ceil(\frac{f_s}{f_{min}}) \tag{42}$$

Where: W_l = data window length in samples

              f_s = sampling frequency

              f_{min} = minimum frequency of interest

              $ceil$ = round up function

The data window, W_l, can be represented as an array of values:

$$mem_{ang} = [B(k - W_l) : B(k)] \tag{43}$$

Where: mem_{ang} = data window for the superimposed angle calculations

A second data window will follow the mem_{ang} window. This data window will contain the difference of angle, $B(k)$, and all values stored within window mem_{ang}. This data window also contains an array of values:

$$mem_{dif} = [B(k) - [B(k - W_l) : B(k - 1)]] \tag{44}$$

Where: mem_{dif} = data window for angle difference calculations

This window is ultimately used to determine the four-count that was previously discussed in Figure 31. The algorithm will evaluate each sign change to determine when a full cycle has occurred. The flow chart below demonstrates the evaluation for the four-count process:
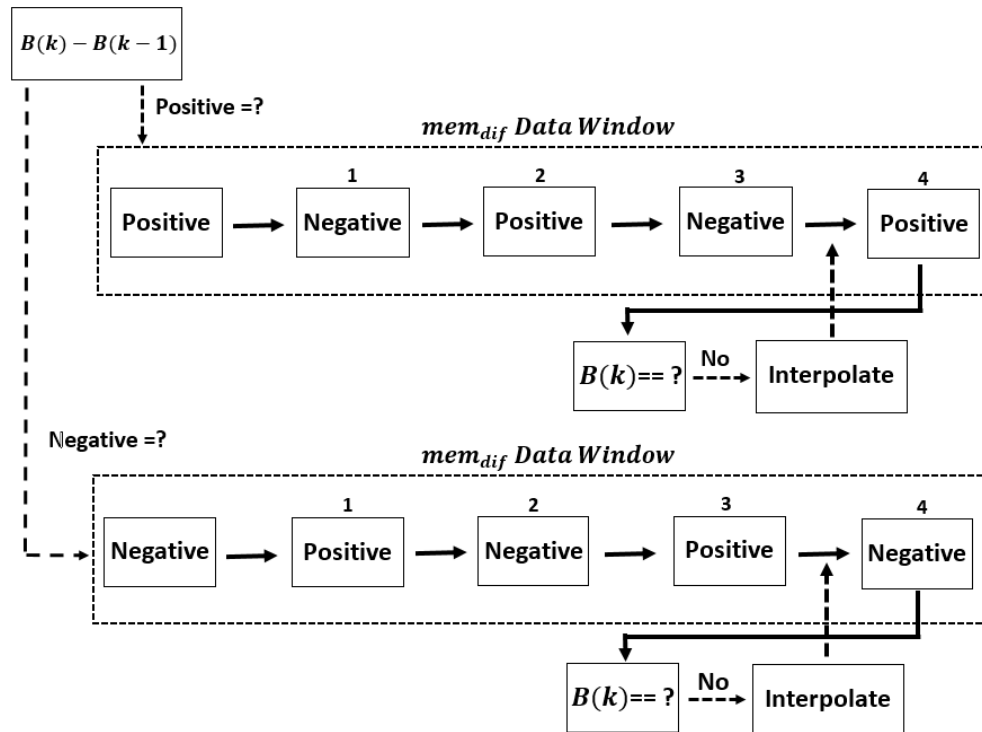
Figure 32: Frequency reporting validation flow chart

The flow chart in Figure 32 starts with the difference of the most recent

established angle, $B(k)$, and the prior assigned angle, $B(k-1)$. If this value is positive,

it evaluates the first transition as the positive-to-negative transition, then looks at each

sign change thereafter until the count reaches four. Similarly, if the difference is

negative, then the method evaluates the first transition as negative-to-positive transition

and considers each sign change that trails until the count reaches four. For either route in

the method, once the transition to the fourth count is established the value is compared to

$B(k)$. If the value does not equal $B(k)$ the method interpolates to find the sample that

occurs at zero. Otherwise, a full cycle occurs on an integer number of samples and

interpolation is not required. There is a corner case where the four-count fails, this is

resolved and discussed following.
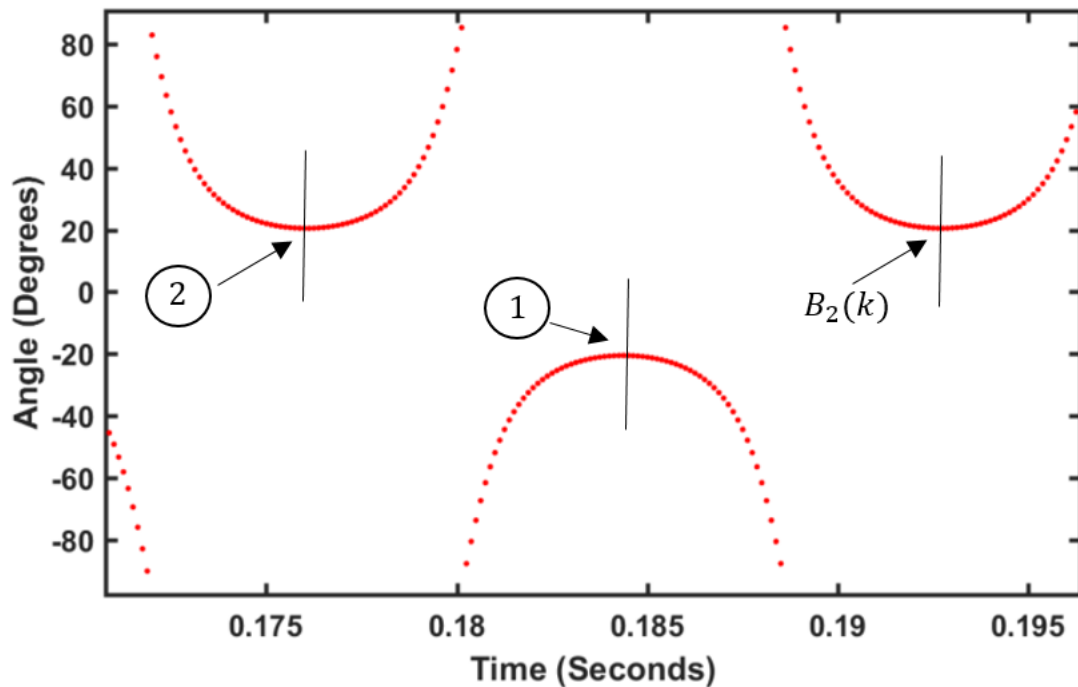
Figure 33: Angle calculation considering four-count fail

The four-count implementation works extremely well, except when the calculated

angle is the minimum or maximum of the function displayed in Figure 33. This does not

impose any issue, in most cases the count would never reach four when the maximum

and minimum does occur. The data window defined by W_l, only contains so many values

in memory. A new frequency value is not updated when the count has not reached four

prior to exceeding the memory of the mem_{ang} data window. If this does reach the four-

count when the minimum and maximum occurs, then the implemented post-filter is relied

upon to remove any false reporting values.

3.1.3 Post Filtering

The implemented post-filtering technique for any frequency method can be vital.

This is the last stage before a value of frequency is reported by the algorithm. The post-

filter will influence the accuracy and limit the rate-of-change-of-frequency to which the

algorithm will respond to. The post-filtering technique for this method is an FIR. As for pre-filtering, the FIR post-filtering will allow for a constant group delay which can be compensated when used for synchrophasor measurements. The type of FIR utilized is a combination of an average and Kaiser window. The Kaiser window is a low-pass FIR filter [27]. Many low-pass FIR filters were experimented with for post filtering and the Kaiser window showed to provide minimal error for all tested waveforms. Two important parameters to consider on the post filter are the filter window length and the cutoff frequency. The chosen post filter length of the average is 50 samples and the Kaiser window is 351 samples, when using a sampling frequency of 8 kHz. The selected cutoff frequency for the Kaiser window is 15 Hz. The post-filter will remove or attenuate any changes in frequency that exceed 15 Hz/s.

3.1.4 BC Frequency Estimation Method – Overview and Flow Chart

The fundamental stages for the proposed frequency method have been discussed. Figures 34 and 35 display an overview of the BC method.
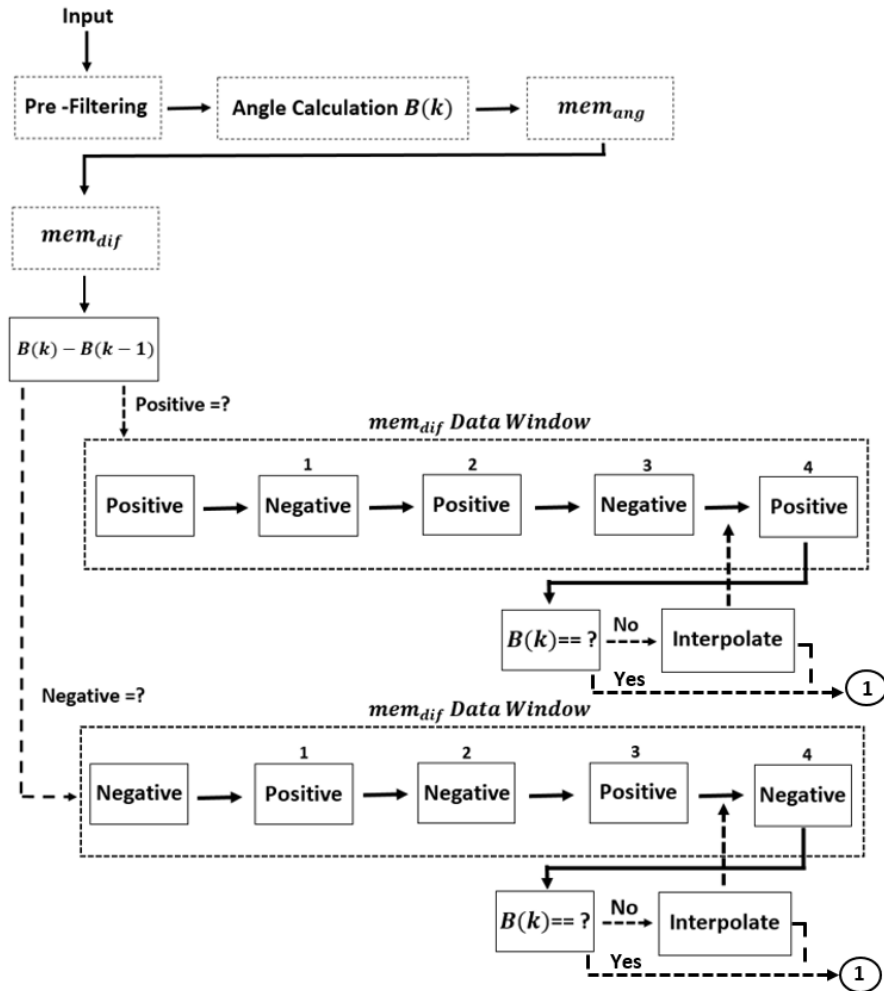
Figure 34: Overview BC method flow chart, part 1

As for any method, the algorithm requires an input signal. For the simulations

and testing within the document, the chosen sampling frequency of the input signal is 8

kHz. The input signal can be voltage or current. The power system consists of three

phases; however, only one phase is necessary for the implementation of this method.

Any phase can be selected. As discussed previously, the input signal will go through the

three-stage average pre-filter.

The angle calculation $B(k)$, is performed on the output of the pre-filtering stage

for each subsequent filtered sample. The $B(k)$ angle calculation requires a *lookback*

value (an integer number of samples prior to sample k) to be selected to perform the

calculations. For the simulations and testing of the BC method within this document, two

$lookback$ values were selected. The selected $lookback$ values were 30 and 60 samples.

These values were selected based on the accuracy displayed when testing several

combinations. Selecting two $lookback$ values improved the associated error imposed

during interpolation. Two angle calculations are performed and both are assigned to the

same sample obtained from the measurement device or coding algorithm. The two angle

calculations are executed in parallel and combined prior to the post-filtering stage. In

other words, the flow chart in Figure 34 is performed twice on each sample.

The difference on the most recent angle calculation $B(k)$, and each value in the

mem_{ang} data window is performed and stored within the mem_{dif} data window. There

are two possible paths the method could route in followed by the difference calculations.

The chosen path is contingent on whether the difference of angle calculations $B(k)$ and

$B(k-1)$, is positive or negative. If the difference yields a negative value, then the next

positive value will start the count at one. Likewise, if the difference results in a positive

value, then the subsequent negative value will start the count at one. For either path,

once the count starts each sign change thereafter will increment the count. The BC

method defines that a complete cycle has occurred after the count reaches four and the

angle at the four-count is evaluated. If the angle at count four is equal to $B_1(k)$, then it is

labeled as $B_2(k)$. This will only occur when there are an integer number of samples for

the measured frequency. If there is not an integer number of samples for the estimated

frequency, then interpolation is required.

When interpolation is necessary, $B_2(k)$ is assigned the interpolated sample

number and angle where the method determines a complete cycle has occurred. Two

interpolation techniques are utilized, quadratic and linear. Quadratic interpolation is computed on three values. The value in the mem_{dif} data window that occurs immediately when the four-count has been satisfied and the two values prior to the four-count in the mem_{dif} window are used for the interpolation calculation. The quadratic interpolation solves for the roots of the equation, if the roots fall inside of the interpolated sample range then the interpolation value is accepted and used for the number of samples/cycle calculation. If the roots fall outside of the samples range, then the interpolated value is rejected and linear interpolation is used. Only two values are utilized for the linear interpolation calculation. Both values are contained within the mem_{dif} window and include the value that occurs immediately on the four-count and the value prior to the establishment of the four-count.

The continuation of the flow chart in Figure 34 can be seen below:
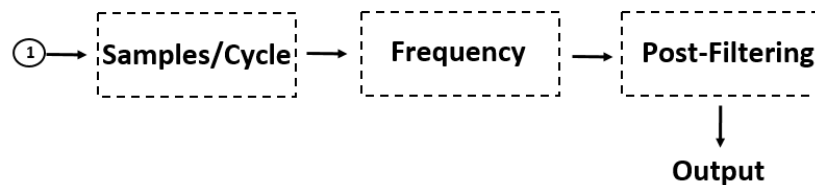
Figure 35: Overview BC method flow chart, part 2

The number of samples/cycle is declared by the difference in the sample that occurs on $B_1(k)$ and $B_2(k)$. Recall, for the simulated measurements in this document two angle calculations were executed in parallel. Therefore, there are two sets of samples/cycle calculated per sample, these two sets are averaged within this stage to combine into a single number of samples/cycle. The number of samples/cycle can be converted to frequency by dividing the sampling frequency by the assigned sample number difference for $B_1(k)$ and $B_2(k)$.

The frequency for this method is updated with each new sample obtained, this is achievable considering each new sample is assigned a new calculated angle. The final stage of the method includes a post-filter. The post-filter combines both an average and Kaiser filter. The average filter is performed prior to the Kaiser window. The addition of the average will decrease the responsiveness of the frequency method. However, the average was included to improve the accuracy of the estimated frequency for amplitude modulated signals. Finally, the Kaiser filter follows the average filter in the method. The implemented Kaiser filter is a low pass filter that defines how fast the method will respond to changes in frequency. The cutoff frequency for this filter was specified as 15 Hz. The output of the Kaiser window is the reported frequency value. This will update at the rate of the sampling frequency of the input signal.

3.1.4 BC Frequency Method Measurement Response

Several signals were mathematically constructed to evaluate the proposed frequency method. The figure below demonstrates a ramp in frequency with a +15 Hz/s ramp rate.
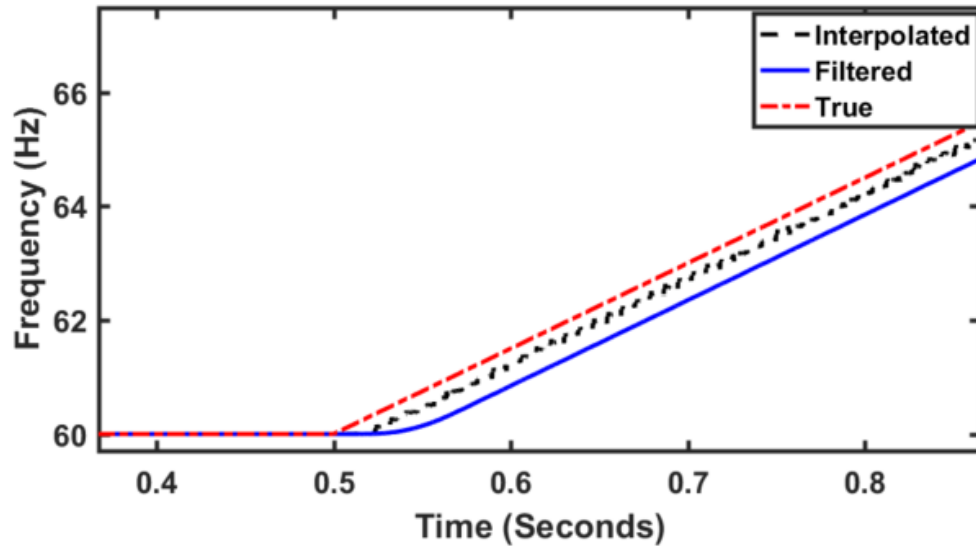
Figure 36: +15 Hz/s frequency ramp response for the BC measurement method

The input signal for the response in Figure 36 pertains to a +15 Hz/s ramp in frequency that occurs when time = 0.5 seconds. The figure displays the true, interpolated, and filtered response. One thing to note is the interpolated signal response does incorporate the pre-filtering stage presented in the BC method and that both the interpolated and filtered signal lag the true frequency signal. This will be inherent for any frequency estimation method, unless the lag is compensated for when applying as a synchrophasor measurement. This measurement lag is contingent on many factors such as: pre-filtering window length and impulse response, frequency computation window length, and post-filtering window length and impulse response. It would be ideal to not have any measurement lag, but at best the measurement lag should be reduced as much as possible so that the response time for the method closely replicates the system frequency when changing. The measurement lag is fixed at 345 samples for the simulated response. This results in a measurement lag of approximately 43 ms, this includes the inherent delay from both pre- and post-filtering. Ultimately, the proposed method responds well

to the constant change in frequency. The figure below illustrates the BC method response to a heavily distorted signal.
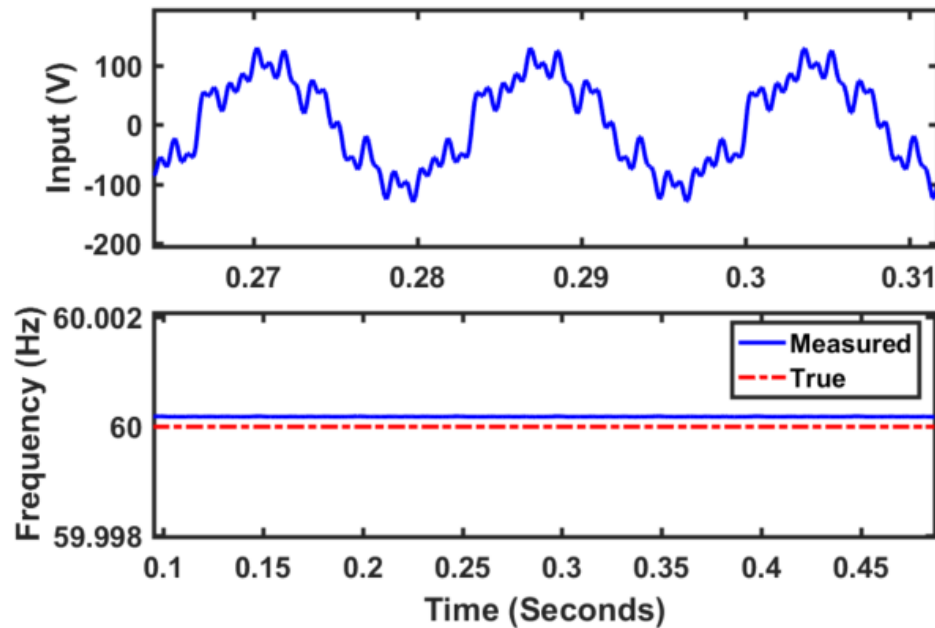
Figure 37: Distorted signal response for the BC measurement method

The input signal in Figure 37 includes four harmonics (5th, 7th, 10th, and 20th) all with a 15 percent magnitude of the fundamental frequency, 60 Hz. The proposed frequency method yielded an error on the order of 0.2 mHz for the simulated input waveform. This shows the method is virtually unaffected by harmonics that are an integer multiple of the fundamental. However, harmonics do not necessarily have to be an integer multiple of the fundamental frequency.

The figure below illustrates the frequency measurement for the BC method when inter-harmonics are included on the input signal.
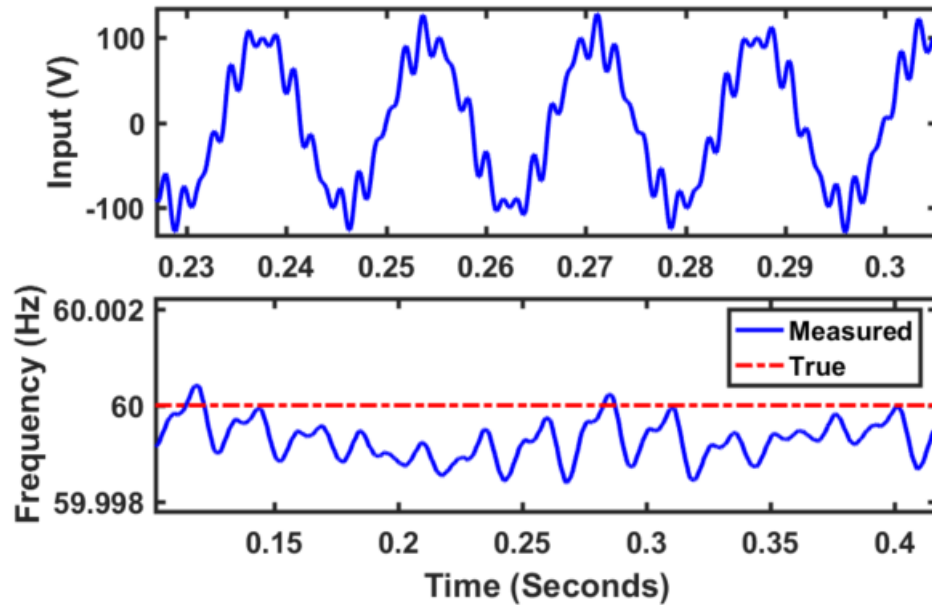
Figure 38: Inter-harmonics signal response for the BC measurement method

The input signal in Figure 38 contains inter-harmonics that are a 7.7 and 10.4 multiple of the 60 Hz fundamental. Both inter-harmonics are 15 percent in magnitude. Notice, the input signal doesn't have any two subsequent cycles that match identically. For the simulated input signal, the measurement method yielded error on the order of 2 mHz. This shows that the accuracy is impacted for the proposed method when inter-harmonics are present; however, the error remains minimal. The presented method yields the largest error when the input signal exhibits an amplitude modulation behavior.
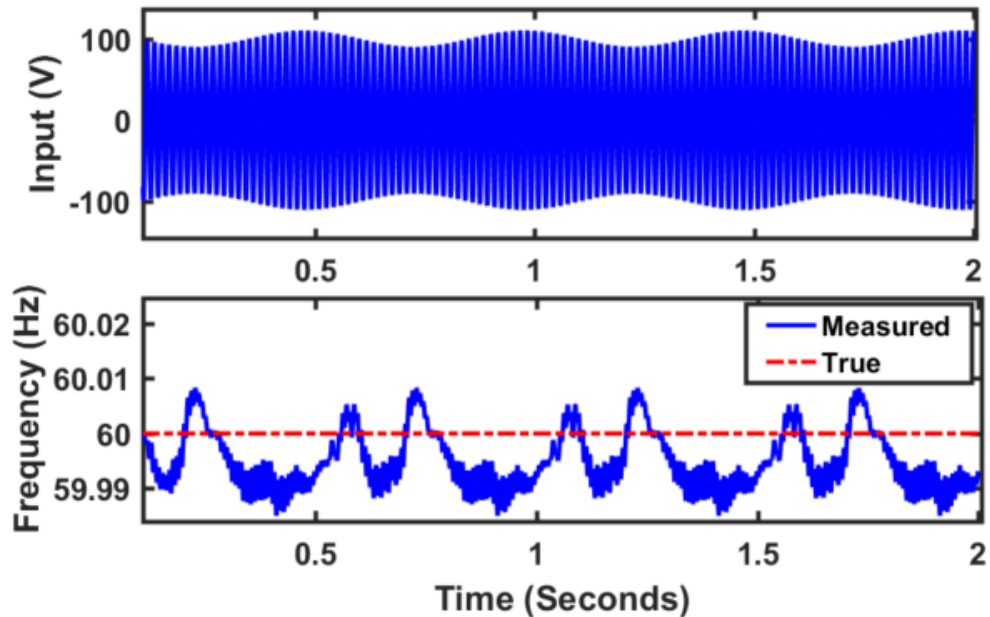
Figure 39: Amplitude modulated signal response for the BC measurement method

The input signal above modulates the waveform at a factor of 0.1 using a modulation frequency of 2 Hz. An amplitude modulated waveform does not vary the fundamental frequency, it only modulates the amplitude of the signal. For the input signal shown in the figure the BC measurement method yields a maximum error on the order of 12 mHz. The error is present because when the angle calculation is performed for an amplitude modulated signal, the angle also exhibits modulation behavior. This signal type is the most problematic for this method; however, the method is still useful for frequency measurements.

Another modulated signal type is phase modulation.
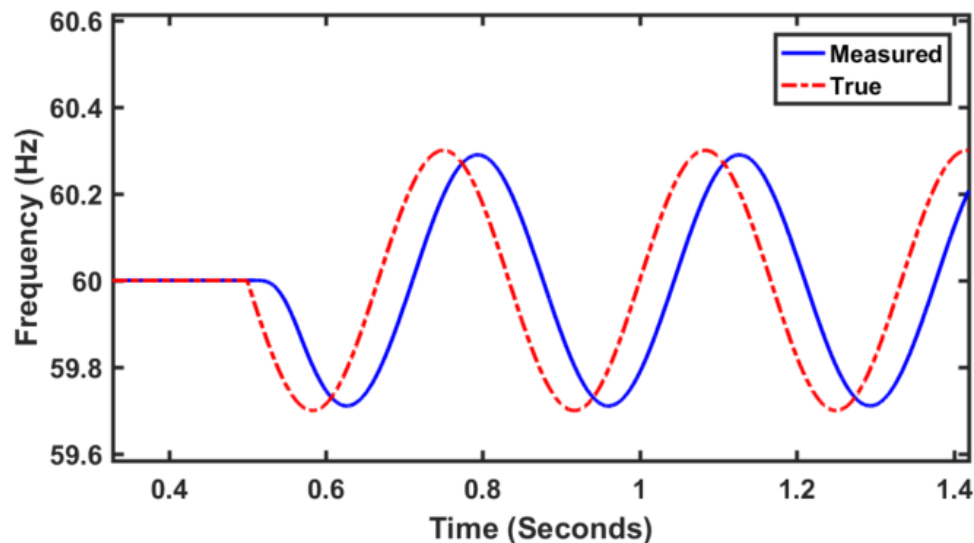
Figure 40: Phase modulated signal response for the BC measurement method

The input signal in Figure 40 is a phase modulated waveform with a modulation factor of 0.1 and contains a frequency modulation of 3 Hz. The accuracy of the BC method is virtually unaffected by a phase modulated signal. As shown in the true signal response, the frequency is varying at a 3 Hz rate and the measured signal maintains the signal response with a known measurement delay (lag).

3.2 Frequency Measurement Testing

Four PMUs that were all IEEE std. C37.118.1a-2014 compliant were tested for the frequency measurement performance. IEEE std. C37.118.1a-2014 compliant devices adhere to the most stringent frequency measurement requirements among standards. Each tested unit was developed from different manufacturers. Each device has been tested individually by the manufacture to comply with the IEEE standard; however, measurement results are not published, they are only listed as compliant. The IEEE std. C37.118.1a-2014 measurements consist of more than just frequency (e.g. phasors, and ROCOF), but only frequency measurements were evaluated for this research. The

purpose of the tests was to evaluate how PMUs from different manufacturers respond with respect to each other for the various test signals.

3.2.1 Tested Signals

To comply with the IEEE std. C37.118.1a-2014, the PMU device must satisfy several measurement verifications [6, 7]. The standard reviews time-tagging and synchronized measurements. The standard also defines several performance tests where limits are specified for compliance verification. Each test consists of a mathematically constructed signal, where the frequency is known throughout the entire duration. The frequency measurement error can be described as [6]:

$$FE = |f_{true} - f_{measured}| \qquad (45)$$

Where: FE = frequency measurement error

f_{true} = true signal frequency

$f_{measured}$ = measured signal frequency

The frequency measurement error calculation applies at the exact instance of time for both f_{true} and $f_{measured}$. Each device was selected to update at 60 frames/sec, along with the M-class performance for the measurement comparison throughout.

3.2.1.1 Steady-State Tests

The first tested waveform is a steady-state signal. Three-phase steady state signals with harmonics can be expressed as:

$$X_A(t) = X_M\sin(2\pi ft) + X_{N1}\sin(2\pi N_1 ft)...+ X_{Nn}\sin(2\pi N_n ft) \qquad (46)$$

$$X_B(t) = X_M\sin(2\pi ft - \tfrac{2\pi}{3}) + X_{N1}\sin(2\pi N_1 ft -$$

$$\tfrac{2\pi}{3})...+ X_{Nn}\sin(2\pi N_n ft - \tfrac{2\pi}{3}) \qquad (47)$$

$$X_C(t) = X_M \sin(2\pi ft + \frac{2\pi}{3}) + X_{N1}\sin(2\pi N_1 ft +$$

$$\frac{2\pi}{3})\ldots + X_{Nn}\sin(2\pi N_n ft + \frac{2\pi}{3}) \qquad (48)$$

Where: X_A = A-phase sample at time = t

X_B = B-phase sample at time = t

X_C = C-phase sample at time = t

f = fundamental frequency

X_M = Amplitude of the fundamental frequency

N_1 = harmonic number

X_{N1} = Amplitude of harmonic number N_1

The steady state tests require the frequency of the fundamental, along with

frequency of each harmonic included, to remain constant. In addition, the amplitude of

all frequency components must stay constant. The standard defines the steady-state error

requirements for compliance as follows [7]:

Table 8: Steady state tests compliance for M-class with reporting rate of 60 frames/s

Signal Specification	Max Frequency Error (mHz)
Fundamental frequency	5
Harmonic distortion	25
Out-of-band interference	10

3.2.1.2 Frequency Ramp Tests

As discussed previously, the frequency of a power system is in a constant state of

fluctuation (typically within +/- 50 mHz); therefore, to correctly monitor the frequency of

the system, the frequency method must also be able to correctly measure the system

frequency during dynamic events. One dynamic event is a ramp in frequency. A

constant ramp in frequency can be characterized mathematically, as shown below [7]:

$$X_A(t) = X_M\cos(2\pi f t + \pi R_f t^2) \tag{49}$$

$$X_B(t) = X_M\cos(2\pi f t - \frac{2\pi}{3} + \pi R_f t^2) \tag{50}$$

$$X_C(t) = X_M\cos(2\pi f t + \frac{2\pi}{3} + \pi R_f t^2) \tag{51}$$

Where: R_f= ramp rate

The ramp rate, R_f, in the above equations is a constant value. The error

requirements for the frequency ramp tests is as follows [7]:

Table 9: Frequency ramp tests compliance for M-class with reporting rate of 60 frames/s

Signal Specification	Max Frequency Error (mHz)
± 1.0 Hz/sec	10

The frequency ramp test consists of a linear ramp in frequency, where f and R_f

are constant. The theoretical frequency can be determined at any specified time for the

given signal by applying the following equation [6]:

$$frequency(t) = f + R_f t \tag{52}$$

3.2.1.3 Amplitude and Phase Modulation Tests

An additional dynamic event that the IEEE standard requires to test for

compliance is a modulated waveform. There are two modulated signal types required for

testing: amplitude and phase modulated. Both signal types are to be tested independent

of one another. The governing equations describe the mathematical representation of the

modulated waveforms [6]:

$$X_A(t) = X_M[1 + \mathrm{k}_a cos(2\pi f_m t)] \cdot \cos[2\pi f t + \mathrm{k}_p \cos(2\pi f_m t - \pi)] \tag{53}$$

$$X_B(t) = X_M[1 + \mathrm{k}_a cos(2\pi f_m t)] \cdot \cos[2\pi f t - \frac{2\pi}{3} + \mathrm{k}_p \cos(2\pi f_m t -$$

$$\pi)] \tag{54}$$

$$X_B(t) = X_M[1 + k_a cos(2\pi f_m t)] \cdot cos[2\pi f t + \frac{2\pi}{3} + k_p cos(2\pi f_m t -$$

$$\pi)] \tag{55}$$

Where: k_a= amplitude modulation factor

k_p= phase angle modulation factor

f_m= modulation frequency

Each modulation test involves selecting k_a, k_p, and f_m for a given nominal

frequency (f). As in the prior dynamic event, the theoretical frequency value for the

above equations can be determined using the following formula [6]:

$$frequency(t) = f - k_p f_m sin(f_m t - \pi) \tag{56}$$

Notice that the above equation does not include the amplitude modulation factor,

k_a, that is used for amplitude modulated signals. The fundamental frequency component

does not vary for amplitude modulated signals; however, this is not the case for phase

modulated signals. The three factors that influence the frequency for phase modulated

signals are the phase angle modulation factor, k_p, the modulation frequency, f_m, and

time. The error requirements for compliance of the modulated signal tests are listed

below [7]:

Table 10: Modulation tests compliance for M-class with reporting rate of 60 frames/s

Modulation Level (radian)	Modulation Frequency (Hz)	Max Frequency Error (mHz)
k_a= 0.1, k_p= 0	$f_m \leq 5$	300
k_a= 0, k_p= 0.1	$f_m \leq 5$	300

3.2.1.4 Phase and Magnitude Step Tests

The last test specified for compliance of the IEEE std. C37.118.1a-2014 is

the input step change. This test will include a step-in phase and/or magnitude. The

fundamental frequency component does not vary for a step-in phase and/or magnitude.

The equations that describe an input step are shown below [6]:

$$X_A(t) = X_M(1 + k_a f_1(t_1)) \cdot \cos(2\pi f t + k_p f_1(t_1)) \tag{57}$$

$$X_B(t) = X_M(1 + k_a f_1(t_1)) \cdot \cos(2\pi f t - \frac{2\pi}{3} + k_p f_1(t_1)) \tag{58}$$

$$X_B(t) = X_M(1 + k_a f_1(t_1)) \cdot \cos(2\pi f t + \frac{2\pi}{3} + k_p f_1(t_1)) \tag{59}$$

Where: k_a = amplitude step size

k_p = phase angle step size

$f_1(t_1)$ = unit step function at time = t_1

The input step change differs from the other tests discussed previously. The

frequency for this condition does not change; however, most frequency estimation

methods will yield a change in frequency value. In some cases, the reported frequency is

far from system nominal. To test the input system, the response time is evaluated as

opposed to frequency measurement error. The response time is defined as, "the time to

transition between two steady-state measurements before and after a step change is

applied to the input [6]." The standard also specifies that the time values and their

difference should only be assigned when the accuracy limits are satisfied for steady-state

compliance [6, 7].

Table 11: Input step tests compliance for M-class with reporting rate of 60 frames/s

Step Change Specification	Response Time (s)
Magnitude = ±10%, k_a= ±0.1, k_p= 0	14/60
Angle = ±10°, k_a= 0, k_p= ± $\pi/18$	14/60

All tests are specified for nominal conditions at the start and end of the input step.

The figure below illustrates how to apply the response time calculation:
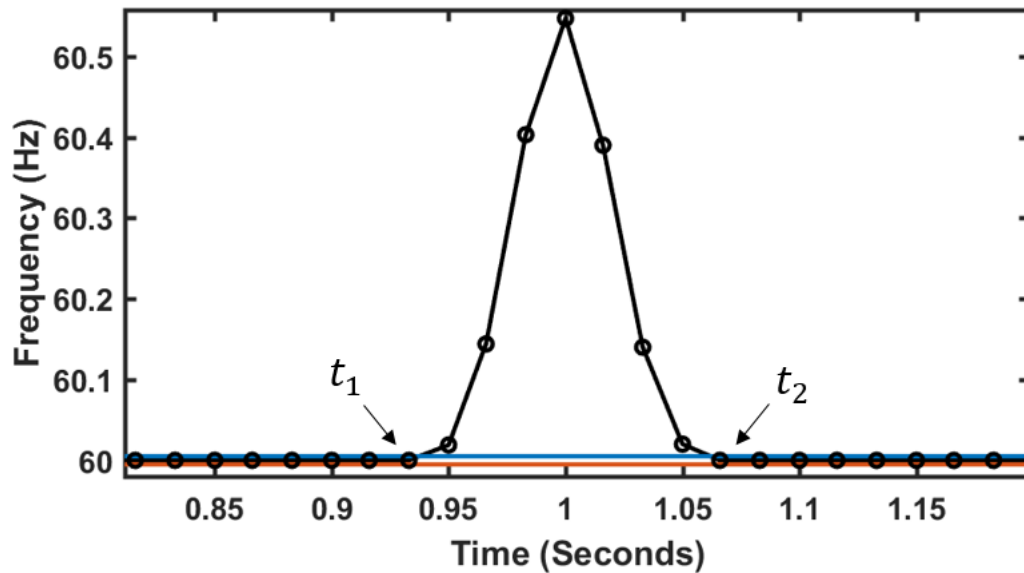
Figure 41: Input step response time

Figure 41 demonstrates a PMU measurement response to a phase angle input step.

Each circle indicates the reported frequency value. The two horizontal lines are the

boundary limits that are specified for a single frequency signal ±0.005 Hz. The time, t_1,

is assigned to the last reporting value prior to exceeding the established limits. Similarly,

the time, t_2, is assigned to the reporting value where the measurement re-establishes

within the steady-state limits. The calculated response time is the difference between the

two times.

3.3 Phasor Measurement Test Procedure

To have full control over the test signals each mathematical expression discussed previously (steady-state, frequency ramp, modulated signals, and input step) were programmed in MATLAB. This allowed for complete control on the amplitude, frequency, phase, and the time for any specific variation of the values.

A code was written, also in MATLAB, to convert the sample values (obtained from the signal equations) to IEEE std. C37.111-1999. This standard is more formally referred to as COMTRADE file format. COMTRADE files are most commonly generated from a PMU triggered event on the power system. This file format stores oscillography, along with binary status, which is a useful tool for analyzing system events [29]. Modern day tests will replay, or replicate the oscillography stored within the COMTRADE file. This allowed for each PMU to be tested using programmed signals to ensure compliancy with the IEEE std. C37.118.1a-2014. The COMTRADE files for all the tested signals were generated using a sampling frequency of 8 kHz.

3.4 PMU Test Setup

Each PMU was tested using a specific layout to maximize the accuracy of the measurements for comparison. The figure below illustrates the test layout for each tested device.
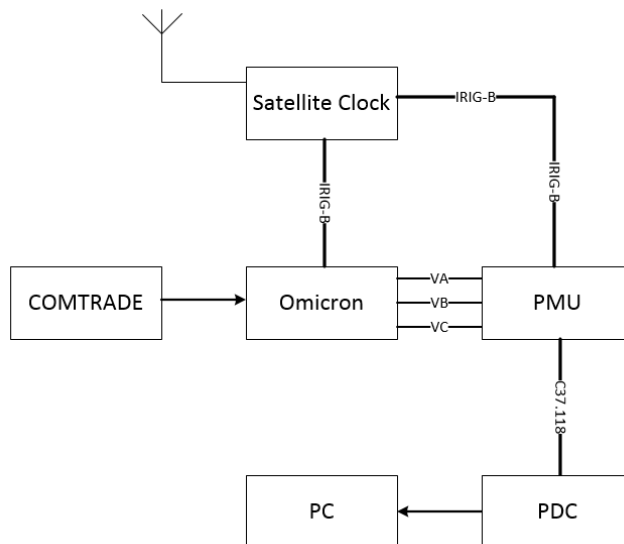
Figure 42: PMU test setup

Figure 42 illustrates the test methodology for the PMU devices. The three-phase

test unit is developed by Omicron. The Omicron test set allows for the reproduction of

COMTRADE stored signals. Each COMTRADE file created, which pertained to a

specific signal type, was loaded in the Omicron for PMU testing. The Omicron was

connected to each PMU using cables that interconnected the voltage outputs of the test

set to the voltage inputs of the tested device.

The test setup required time synchronizing each PMU so that the measurements

could be compared with respect to an absolute time. Figure 42 shows that a GPS satellite

synchronized clock is connected to both the Omicron and the PMU under test. The

Omicron was selected to replay each event on the top of the second. Each PMU was

tested independently, so on the top of second (specified within the Omicron test set) for

the replay of the event, was used as the origin for the measurement comparison of the

devices. To further describe this concept, consider any signal and assign a name, the

illustration signal is as Signal-1. Signal-1 was applied to each of the tested units;

however, at unique times. The replay time for Signal-1 on each unit is as follows: PMU1

= 12:00:00, PMU2 = 12:36:00, PMU3 = 13:58:00, and PMU4 = 15:36:00. The time at

which the signal was applied will be considered time = 0 for the measurement

comparison, or in other words, the origin for each device. This allows each PMU device

to have a common origin and they can be compared against each other with accuracy

specified by the test set and clock manufacturer.

The testing equipment, along with associated error specifications is listed below:

Omicron CMC 256 plus [30]

Error < 0.015% reading + 0.005% range

Range = 150V

Resolution < 5 μs

CMIRIG-B interface [31]

Typical = ± 1μs, Maximum = ± 5μs

SEL-2407 Satetillite Synchronized Clock [32]

Average = ± 100 ns, Maximum = ± 500 ns

The measured data from each PMU is passed to a local phasor data concentrator

(PDC) using C37.118 communication protocol. The PDC was software based, so that all

the reported data from each PMU could be stored directly to the local computer (PC) for

analysis.

3.5 BC Method Test Procedure

The BC method has been introduced in this document and the goal of this work is

to not only compare the frequency measurements among the available PMU devices, but

also compare the measurements from the new proposed BC method as well. The BC

method is not yet implemented in hardware, so the procedure to compare this method with respect to each of the units will differ from the testing of the PMUs.

As previously mentioned, COMTRADE files are commonly stored within a PMU device to record the system's voltage and current. This feature was utilized to test the measurement accuracy of the BC method. For each tested signal, a COMTRADE file of the measured samples was stored by a PMU. These data are the actual obtained samples from the PMU under test. Using the samples obtained from the PMU will allow the BC method to be compared against the PMU frequency measurements as if it were also implemented in hardware instead. As oppose to just comparing the measurements with ideal MATLAB samples. Ultimately, the samples archived by the PMU (within the COMTRADE file) include any slight A/D error and noise embedded in each value. The BC method has successfully been implemented within MATLAB code. Each COMTRADE file stored from the tested PMU will correspond to a specific signal type. Each file is placed into MATLAB so that the BC algorithm will execute measurements for each signal type stored within the PMU. The COMTRADE file not only stores the measured data sample, but also the timestamp at which it was obtained. This allows the BC method to be compared directly against the other PMU while maintaining the timing accuracy that was presented in the equipment specifications.

CHAPTER 4: RESULTS

4.1 PMU and BC Method Measurement Results

This sections reviews the frequency measurements obtain from each of the four

PMUs, along with the BC frequency method. The IEEE std. C37.118.1a-2014 requires

extensive testing for a PMU to achieve compliancy. Each tested unit has already been

determined to meet the IEEE requirements, so only selective tests were performed to

determine how the accuracy matches up against the other three PMUs. In addition, the

measured response for the BC method is also compared against the four PMUs.

4.1.1 Steady-State Results

The first tested signal is to determine the accuracy of the frequency measurements

throughout steady-state conditions. As shown earlier, the steady-state signal

representation for a single phase is shown below:

$$X(t) = X_M \sin(2\pi f t) + X_{N1} \sin(2\pi N_1 f t) \ldots + X_{Nn} \sin(2\pi N_n f t) \qquad (60)$$

Recall, for a steady-state waveform, the amplitude and frequency remain constant

throughout the duration of the signal. Three steady-state waveforms were performed for

testing; the waveform types are listed below:

Table 12: Steady state tests

Test #	Amplitude, X_M (V)	Fundamental Frequency, f (Hz)	Harmonics Order, N	Harmonics Amplitude, X_M (V)
1	100	60	-	-
2	100	60	2, 3, 4, 5	10 for each
3	100	60	20	10

Each of the three tests was ten seconds in length. The error calculation was executed from the 1-9 seconds' time span. It will take time for a frequency algorithm to settle at a valid reporting value after initially applying a signal. Starting the error calculations at 1-second allowed each PMU, along with BC method, sufficient time for optimal performance. The steady state test responses are shown in the figures below:
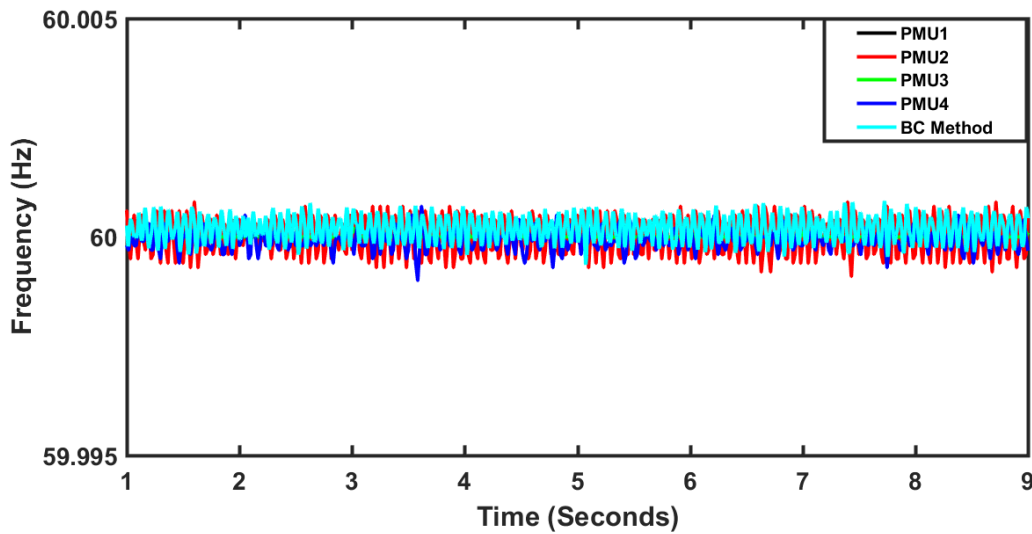
Figure 43: Steady-state frequency response – Test 1

Figure 43 displays the measurement responses for each of the PMUs, including the BC method. Notice, the y-axis is limited at ± 5 mHz, this is the corresponding limits established by the IEEE standard for a signal frequency injection test.

Figures 44 and 45 show the measured responses when including one or more harmonics superimposed on a fundamental frequency component.
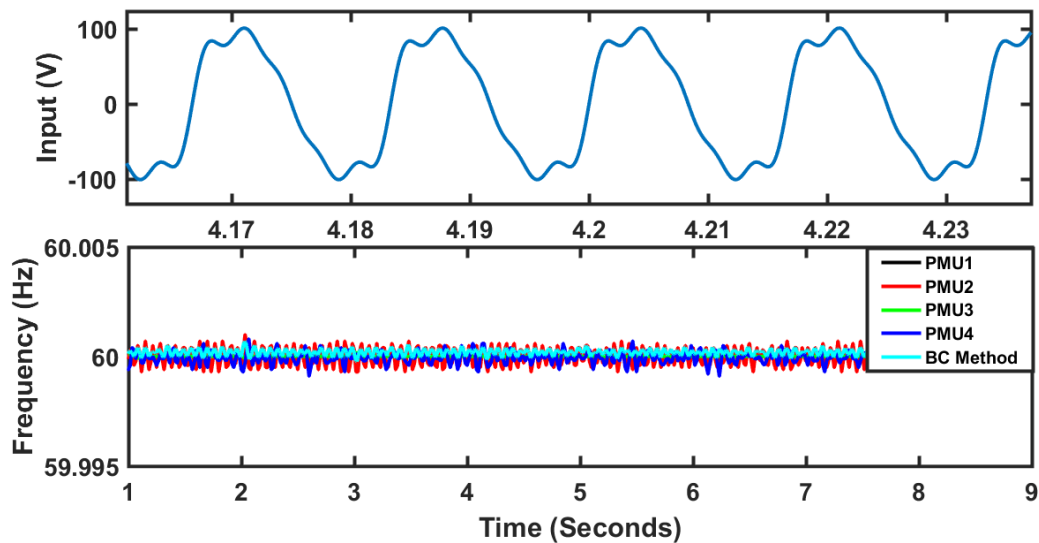
Figure 44: Steady-state w/harmonics frequency response – test 2
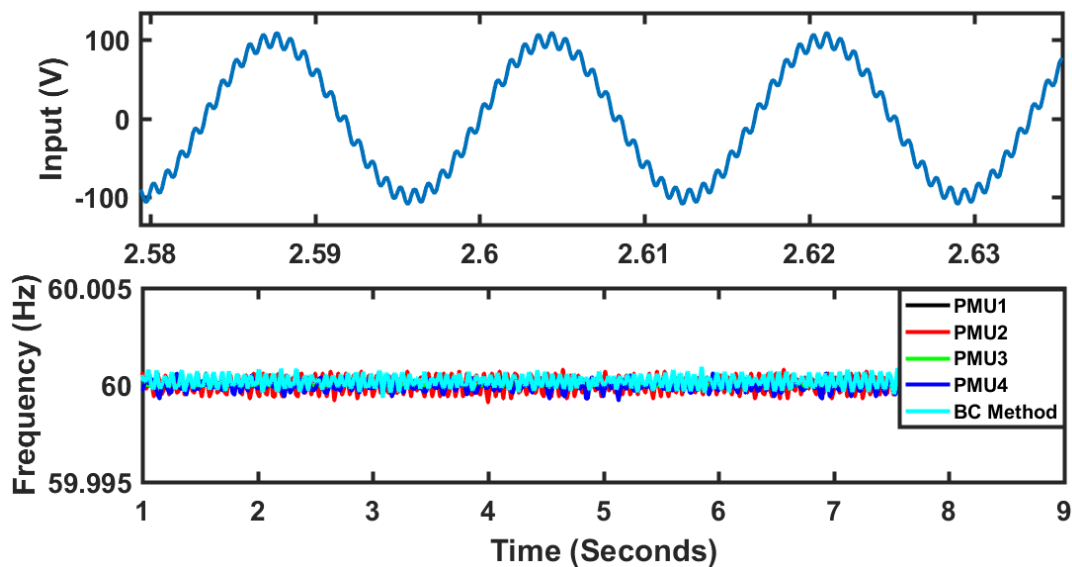
Figure 45: Steady-state w/harmonic frequency response – test 3

The IEEE standard widens the error limits for a steady-state frequency that includes harmonic distortion; however, the measured responses show that all comply within the ± 5 mHz frequency limits.

The corresponding frequency error measurements are listed in the table below:

Table 13: Steady state maximum frequency error (mHz)

Test #	PMU 1	PMU 2	PMU 3	PMU 4	BC Method
1	0	0.9	0.2	1.0	0.8
2	0	1.0	0.2	0.9	0.7
3	0	0.9	0.2	0.8	0.9

The results in Table 13 show that all measurements comply with the standard, as expected, including the BC method. The measurement error, for each performed test, ranged from 0-1 mHz.

4.4.2 Frequency Ramp Results

The next signal type that was tested is a linear ramp in frequency. A ramp in frequency for a single phase, as listed earlier, is expressed as:

$$X(t) = X_M \cos(2\pi f t + \pi R_f t^2) \tag{61}$$

The IEEE standard only specifies for ± 1.0 Hz/s ramp rates to be tested; however, additional tests were performed outside of signal specification. The table below lists the tests that were performed for a ramp in frequency:

Table 14: Frequency ramp tests

Test #	Amplitude, X_M (V)	Fundamental Frequency, f (Hz)	Ramp Frequency, R_f (Hz/s)	Signal Length (s)
1	100	60	+0.5	11
2	100	60	-0.5	11
3	100	60	+1	6
4	100	60	-1	6
5	100	60	+3	4
6	100	60	+5	2
7	100	60	+10	1.5
8	100	55	+15	1.5

The injected signal lengths varied dependently upon the frequency ramp rate, R_f, tested. The signal lengths are listed within the Table 14. Just as before, one second was allowed for each unit and method to adjust to optimal reporting values. Therefore, one second of steady state frequency, f, was included prior to the ramp initiation of the ramp in frequency. Per the standard, there is an allowance for the transition time to ramp in frequency [6, 7], which allows two reporting rates to be discarded from the error calculations. Therefore, the error calculations started at 1.05 seconds for all tested signals. The end time for each error calculation is included within the table. Figure 46 below displays the frequency measurement responses for a ramp in frequency:
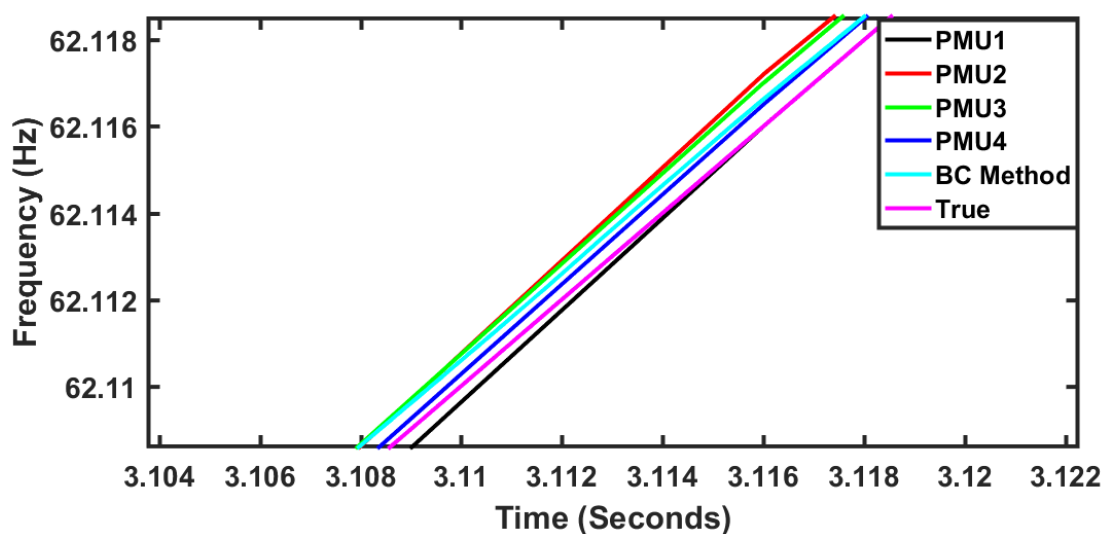
Figure 46: Frequency ramp test +1Hz/s

It also shows the graphed results of the +1Hz/s frequency test. All responses, for this test, are within 0. 5 mHz from each other. One thing to keep in perspective here, the true frequency is also graphed with the results. Notice, in some cases the PMUs and BC method is leading the true system frequency. As mentioned previously, the time-tagging of the frequency value can be influenced by many factors and give the appearance as if the measured frequency is responding faster than the system. This is certainly not the

circumstance; however, it is clear that the units are very accurate with respect to the true frequency and one another. The maximum frequency error for each of frequency ramp tests are displayed in the table below:

Table 15: Frequency ramp maximum frequency error (mHz)

Test #	PMU 1	PMU 2	PMU 3	PMU 4	BC Method
1	1.5	1.3	0.7	1.0	0.8
2	1.0	1.1	0.7	1.0	1.0
3	1.0	1.5	1.2	1.2	1.0
4	1.0	1.5	1.3	1.2	1.3
5	2.0	2.9	3.4	3.0	3.4
6	2.0	4.3	6.7	4.0	2.1
7	4.0	7.8	10.9	7.5	3.0
8	11.0	11.5	17.9	10.9	5.7

Table 15 shows that each PMU tested, along with BC Method, adhered to the error guidelines within the IEEE standard. The standard lists the error requirements must be within 0.01 Hz for a ±1 Hz/s ramp rate. Tests 3 and 4 include the specified ±1 Hz/s ramp rate, the measurement errors ranged between 1-1.5 mHz for these two tests. These values well surpass the error requirements for compliance. In fact, for tests 1-6, with a maximum ramp rate of +5 Hz/s, all units are within the specified error range. The BC method was the only measurement that met the error requirements (< 0.01 Hz) up to a 15 Hz/s ramp rate. This is likely because the cutoff frequency for the PMU devices was selected below 15 Hz.

4.4.3 Amplitude and Phase Modulation Results

The next tested dynamic events are modulated signals. Both amplitude and phase modulated signals are considered; however, each modulation type is tested independently. For reference, the modulated waveform for a single phase is expressed mathematically as shown below:

$$X(t) = X_M[1 + \mathrm{k}_a cos(2\pi f_m t)] \cdot cos[2\pi f t + \mathrm{k}_p \cos(2\pi f_m t - \pi)] \quad (62)$$

First, the amplitude modulated tests were performed, which involved specifying

the amplitude modulation factor, k_a, and increasing the modulation frequency, f_m, up to

5 Hz. Similarly, the phase modulation test was executed by selecting the phase angle

modulation factor and incrementing the modulation frequency. To follow the standard,

the PMU manufacturer must test using a modulation frequency range of 0.1-5 Hz with

steps of 0.2 Hz or smaller. However, as mentioned previously, for these tests only

specific values were chosen for analysis. The performed amplitude modulated tests are

listed below:

Table 16: Amplitude modulation tests

Test #	Amplitude, X_M (V)	Fundamental Frequency, f (Hz)	Amplitude Modulation Factor, k_a	Modulation Frequency, f_m (Hz)
1	100	60	0.1	0.1
2	100	60	0.1	1
3	100	60	0.1	2
4	100	60	0.1	3
5	100	60	0.1	4
6	100	60	0.1	5

The input signal and measurement responses for an amplitude modulated

waveform are seen below for Test #6:
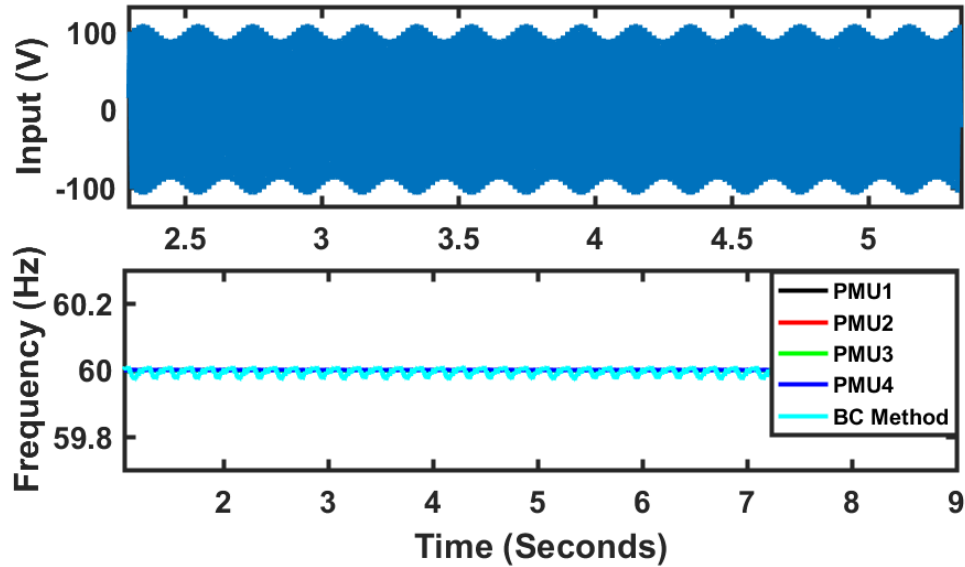
Figure 47: Amplitude modulation test including 5 Hz modulation at k_a=0.1

In Figure 47, the y-axis limits were set on the frequency plot to adhere to the error guidelines established within the standard ± 300 mHz. The fundamental frequency component does not change for an amplitude modulated signal. The measurement error results for the tested devices and BC method are listed below:

Table 17: Amplitude modulation maximum frequency error (mHz)

Test #	PMU 1	PMU 2	PMU 3	PMU 4	BC Method
1	0	0.8	0.2	0.8	2.9
2	0	0.8	0.2	0.9	17.2
3	0	0.9	0.3	0.9	15.1
4	0	0.9	0.6	0.9	40.4
5	0	1.2	1.0	0.9	40.6
6	0	1.6	1.5	1.1	30.9

All tested PMUs perform within 0-1.6 mHz for all tests; however, the BC method performed far outside this range. The worst measured error for the BC method was 40.6 mHz. Although, the measured value is approximately 40 mHz from nominal, this is well within the standard specification of 300 mHz.

The phase modulated tests are listed as follows:

Table 18: Phase modulation tests

Test #	Amplitude, X_M (V)	Fundamental Frequency, f (Hz)	Phase Modulation Factor, k_p (radians)	Modulation Frequency, f_m (Hz)
1	100	60	0.1	1
2	100	60	0.1	2
3	100	60	0.1	3
4	100	60	0.1	4
5	100	60	0.1	5

The phase modulated waveform does not vary in amplitude, but the frequency does vary at a sinusoidal variation. The measured response for a phase modulated waveform in Test #5 is shown below:
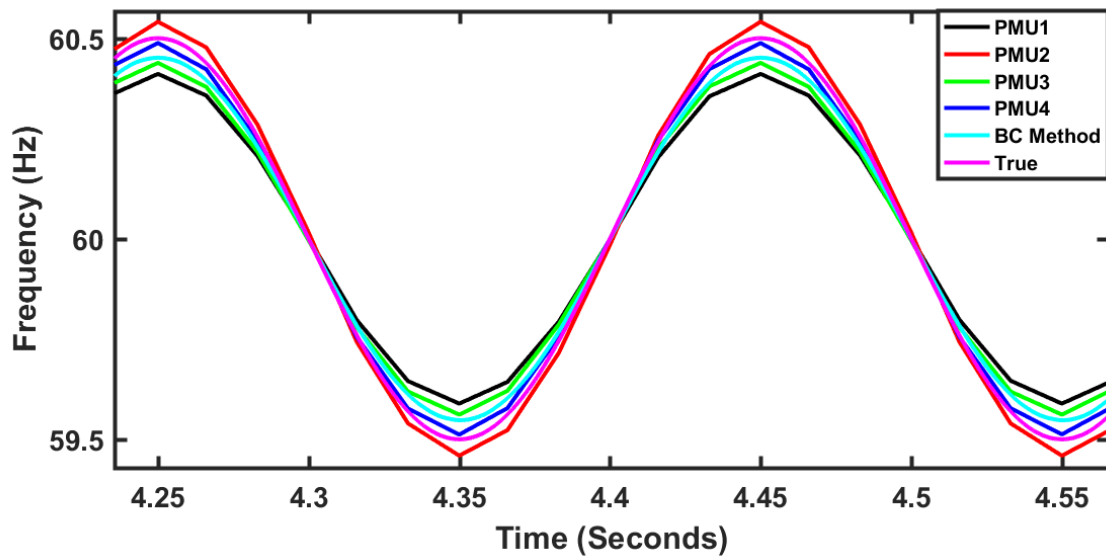

Figure 48: Phase modulation test including 5 Hz modulation at k_p=0.1

In Figure 48, PMU2 and PMU4 show to measure closest to the true frequency. Notice the frequency response for PMU1 and PMU3 with respect to the true frequency where, the signals are properly aligned; however, the measured frequency is attenuated. This is the side effects of extensive filtering and/or data window length.

The frequency error for all phase modulated test cases are shown below:

Table 19: Phase modulation maximum frequency error (mHz)

Test #	PMU 1	PMU 2	PMU 3	PMU 4	BC Method
1	1.9	1.2	0.9	1.3	1.0
2	7.0	3.6	5.1	2.5	2.8
3	21.0	10.4	14.8	4.9	5.4
4	47.5	23.6	32.8	9.3	11.0
5	89.0	47.7	61.6	16.4	49.1

The measurement responses range from 0. 9 – 89.0 mHz for all PMU units,

including the BC method. Test-5 showed the most challenging for all the units with a

range from 16.4 – 89.0 mHz. All measurements satisfy the compliance guideline of 300

mHz. The phase modulated tests showed the widest variation in measurements thus far.

4.4.4 Phase and Magnitude Step Results

The final test for compliance consists of an input step in magnitude or phase. For

convenience, the equation that describes an input step is displayed below:

$$X(t) = X_M(1 + k_a f_1(t_1)) \cdot \cos(2\pi f t + k_p f_1(t_1)) \tag{63}$$

As mentioned previously, the frequency error calculation does not apply for input

steps. The maximum response time is used to evaluate the PMU. The standard specifies

for the input step to be applied on the reporting time and subsequent times increasing in

fractions of the reporting time. Overall, the combination of the response times would be

a comparable step response measurement. This sequence of testing was not carried out to

this degree. There are four independent step tests performed, these are listed below:

Table 20: Phase angle and magnitude step tests

Test #	Amplitude, X_M (V)	Fundamental Frequency, f (Hz)	Phase Angle Step Size, k_p (Deg.)	Amplitude Step Size, k_a (%)	Step Time, t_1(s)
1	100	60	10	0	1
2	100	60	90	0	1
3	100	60	0	10	1
4	100	60	10	10	1

The standard only specifies Tests #1 and #3, but a 90-degree phase step was included for Test #2. In addition, the amplitude and phase step was combined no Test #4 for testing. The BC method is not programmed to decimate the data for C37.118 reporting times on the succeeding graphs; however, the data was decimated properly for the response time calculations for easy comparison.
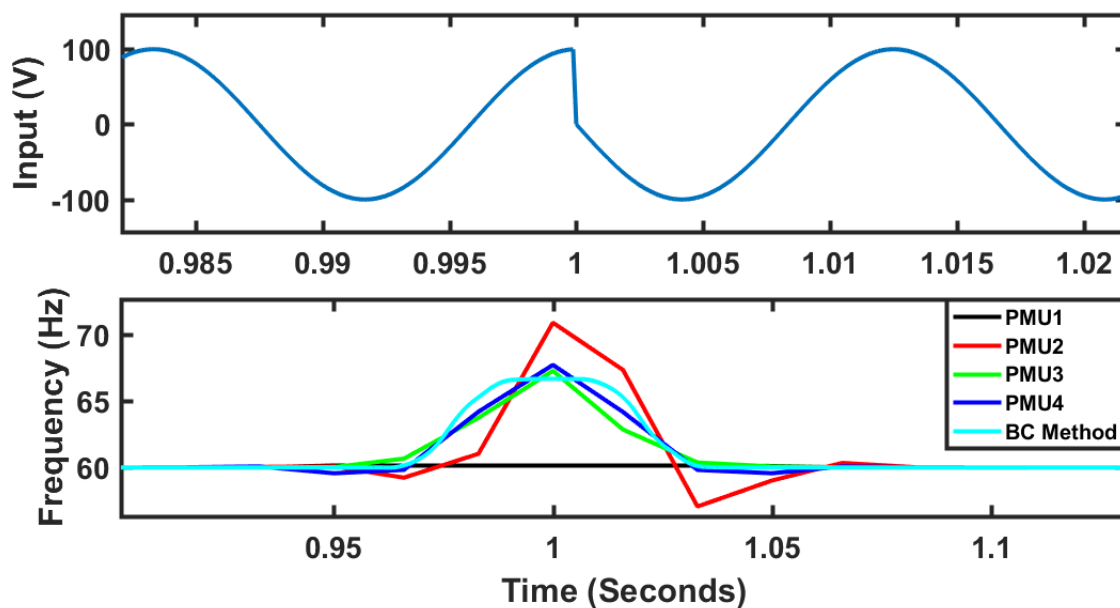


Figure 49: Phase angle step with90 degrees step size

Figure 49 illustrates that the responses are at their maximum when the step occurs. Also of note is that the input step occurs when time = 1 seconds; however, each of the PMUs respond before the event. This is the effect of the window data length. For

instance, if the frequency data window is 8 cycles in length, then the estimator will report

invalid values of frequency until 8 cycles after the event occurs. At this point the phase

step will no longer be evaluated; however, recall for time stamping applications (such as

C37.118.1a-2014) the data will be time stamped at the center of the window. Therefore,

the device appears to predict the input step response, when in fact it does not.

A similar outcome is seen from a magnitude step input as shown below:
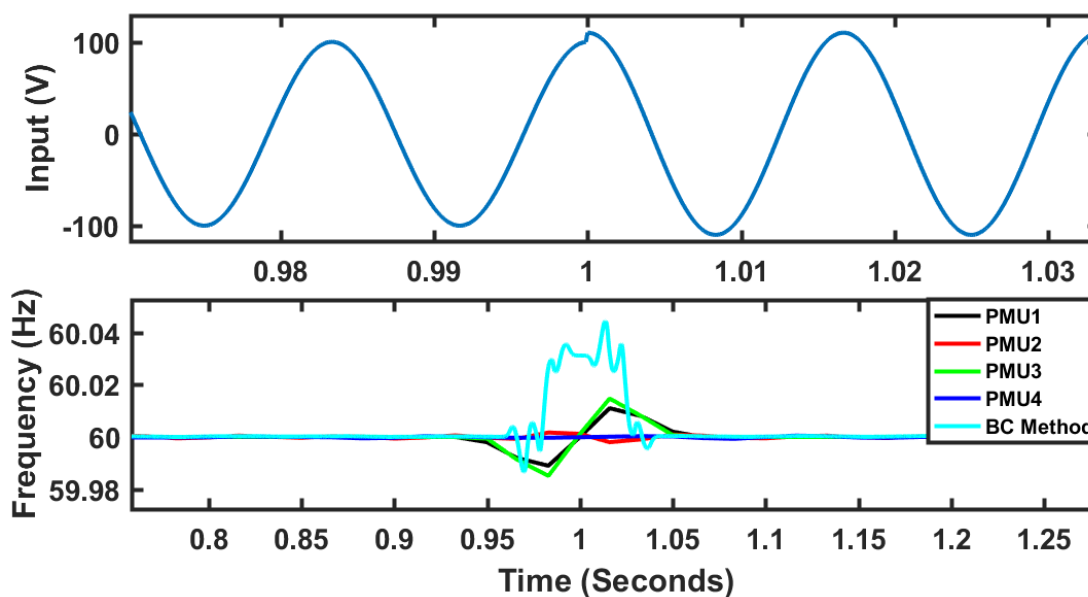
Figure 50: Magnitude angle step w/10% step size

The response times are included within the table below:

Table 21: Phase and/or magnitude step response time (s)

Test #	PMU 1	PMU 2	PMU 3	PMU 4	BC Method
1	0.133	0.167	0.100	0.167	0.100
2	0.133	0.200	0.133	0.200	0.100
3	0.100	-	0.100	-	0.067
4	0.133	0.167	0.100	0.167	0.100

Each device, including the BC method, showed to have very similar response

times. All response times are within requirements for compliance.

4.4.5 System Event Test Results

All tested PMU devices and the new proposed frequency estimation method have

been shown to meet the requirements for the reviewed test conditions.   All devices were

shown to have minimal error under test conditions. One last test was performed on each

of the PMUs, which involved a true power system frequency excursion event on a 60 Hz

nominal system. The digital samples for the event were stored within the local relay at a

sampling rate of 128 samples/cycle. The event was interpolated at a fixed 9 kHz

sampling frequency using the Omicron Test Universe software. This allowed for pre-

frequency excursion data to be added easily. The measured frequency response can be

seen below:
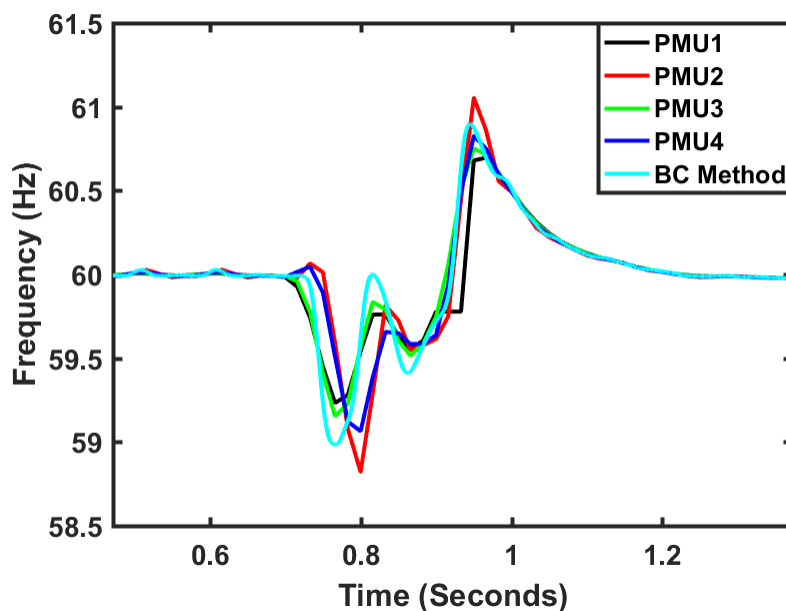

Figure 51: Replayed system frequency excursion

Figure 51 displays the measured frequency response for each PMU, along with

BC method. The response for each of the PMUs differ during the frequency excursion.

There is no reference signal to compare to, like on the other test scenarios; therefore, the

only way to gauge the measurements is to how they compare to one another. To further

quantify the difference in measurements the difference was taken of the maximum and minimum reported at each reporting instance. The BC method was excluded from the evaluation. The figure below graphs the maximum frequency difference for each corresponding reporting measurement.
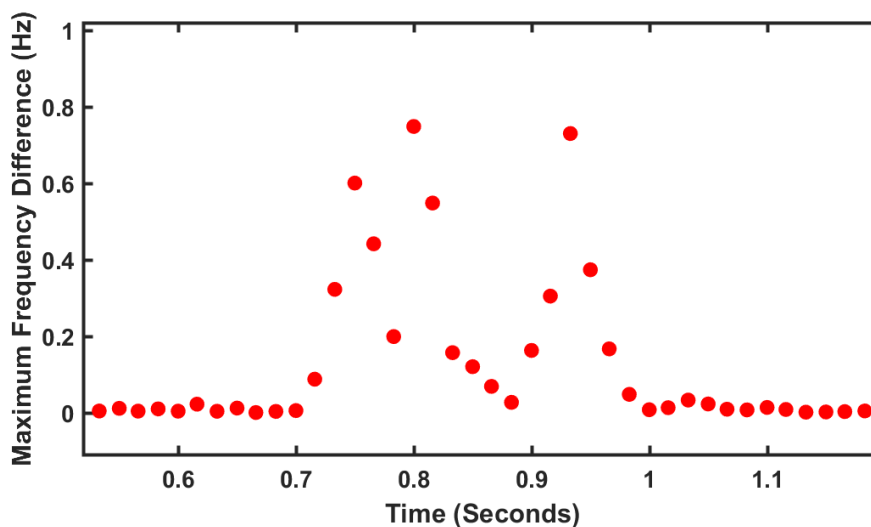
Figure 52: Replayed system frequency excursion

The graph yields that the maximum reporting difference is 748.3 mHz at a reporting time of 0.8 seconds into the replayed event. The maximum reporting difference, via test scenarios, was 72.6 mHz. The reporting difference for this event yielded an order of magnitude difference when compared to the worst case, via IEEE test conditions.

It is probable that a step-in phase and/or magnitude occurred prior or during the frequency excursion, this would explain the large differences shown in the graph. However, this further illustrates that true dynamic events challenge the definition of power system frequency and how measurements are applied in the field.

CHAPTER 5: CONCLUSION

5.1 Discussion

The intent of this research consisted of two main parts. The first portion was to

provide a better understanding for the importance of power system frequency and attempt

to provide an alternative method for measuring frequency throughout the power system.

The goal was to create a simple, yet fast measurement method where the reporting rate

was only limited by the processing capability of the implemented device and sampling

rate of the discrete signal. The new proposed frequency measurement method showed

promising results. The BC method takes a relatively simple approach. Looking back at a

high-level definition of frequency: it is explained as the rate of occurrence. The BC

method superimposes an angle calculation on an arbitrary signal and counts the number

of occurrence. Once the count cumulated to a value of four, then a full power system

cycle was declared. This method doesn't require an extensive knowledge of

mathematics; this would allow for an effective and easy implementation when in

hardware. By counting to four and applying Pythagorean theorem a plausible method

was developed. The benefit of this method is no specific event (e.g. zero-crossing) is

required. It uses a single cycle data window to determine frequency and has the

capability of reporting a new frequency value at the rate of the ADC. This allows the

method to run in the background on a platform and report a value of frequency at a user

selectable rate. A simple pre-filtering method was implemented to improve accuracy for

noisy environments. Additionally, a Kaiser window was added as a post filter to offer

better responses for signals containing inter-harmonics and amplitude variations. Both

filters introduce a linear group delay allowing for easy implementation for time-tagging

applications.

The second portion was to determine the range of frequency error that applied to

PMUs across different manufacturers. Throughout the power system there are protective

relays with PMU functionality, in addition to standalone PMUs. These PMUs are created

from several different manufacturers. The industry would like for all units to perform

similarly. Therefore, standards such as IEEE std. C37.118.1a-2014 are put into place. To

get a better understanding of possible inconsistencies between various manufactured

PMUs, four units were tested. Additionally, the new proposed frequency method was

also tested against the different PMU responses. The tests incorporated the use of a

three-phase test set (Omicron) to replay COMTRADE files that consisted of the IEEE

std. C37.118.1a- 2014 defined test signals. Each PMU tested was certified compliant

with the IEEE std. C37.118.1a- 2014. A portion of the standard requires the device under

test to measure frequency within specified limits to ensure accuracy. In addition, the BC

method was tested in MATLAB using several signal types (stored in COMTRADE file

format) that were obtained by a local PMU when performing the IEEE std. C37.118.1a-

2014 conformance testing.

Each PMU is developed from different manufactures who employ highly

proprietary methods to determine the value of frequency for the power system. The

devices proved to responded similar with respect to frequency error. The point of the

research is not to highlight that a single manufacturer is better than the rest, it is to surface the need for a common definition of frequency.

1. The steady-state tests as comprised of a 60 Hz fundamental signal and included harmonics of various order. The four PMUs measured a range of frequency error between 0 – 1.0 mHz for the tested steady-state signals. The largest inconsistency measured was 1 mHz. In addition, the BC method yielded error in the range of 0.7 - 0.9 mHz for the steady-state tests.

2. The frequency ramp tests included ramps in frequency from 0.5 – 15 Hz/s. The IEEE std. C37.118.1a- 2014 only requires testing +1 Hz/s and -1 Hz/s waveforms; however, the additional tests outlined possible inconsistencies when connected to an actual power system. For the +1 Hz/s and -1 Hz/s frequency ramps, the PMUs responded with an error range of 1.0 – 1.5 mHz. The BC method resulted in error from 1.0 – 1.3 mHz for the same signal types. When evaluating all tests including a ramp in frequency the error ranged from 0.7 – 11.5 mHz for the PMUs and 0.8 – 5.7 mHz for the BC method.

3. The amplitude modulated tests consisted of an amplitude modulation factor of 0.1 and frequency modulation range of 0.1- 5 Hz. The four PMUs measured error within 0 – 1.6 mHz. However, the BC method measured error in the range of 2.9 – 40.6 mHz. The largest inconsistency between the BC method and the PMUs was during amplitude modulated signals.

4. The phase modulated tests were comprised of 1 – 5Hz of phase modulation using a modulation factor of 0.1. The PMUs yielded error within 0.9 – 89.0 mHz for the tested signals and the frequency error for the BC method ranged from 1.0 –

49.1 mHz. The largest measurement inconsistency occurred during phase

modulated signals for the four tested PMUs.

5. The last tests included an input step in magnitude and/or phase angle. The step

tests included a 10-degree and 90-degree phase angle step, 10% magnitude step,

and a combination of a 10-degree phase angle step with an increase in magnitude

by 10%. The input step tests were evaluated using response time as oppose to

frequency error. The response time for the PMUs ranged from $0 – 0.2$ seconds.

The response times for the BC method ranged from $0.067 – 0.1$ seconds.

The response time during an input step, along with all frequency error

measurements were all within the IEEE std. C37.118.1a- 2014 requirement guidelines.

No single unit outperformed the rest in every performed test. Certain PMUs performed

better under certain varying conditions and vice versa. The most unsettling

measurements pertain to an input step in phase angle and/or magnitude. Although each

PMU is clearly in boundary for compliance and reporting response times between 0.1-0.2

s. The frequency error in these scenarios is most erratic. Consider the following graph:
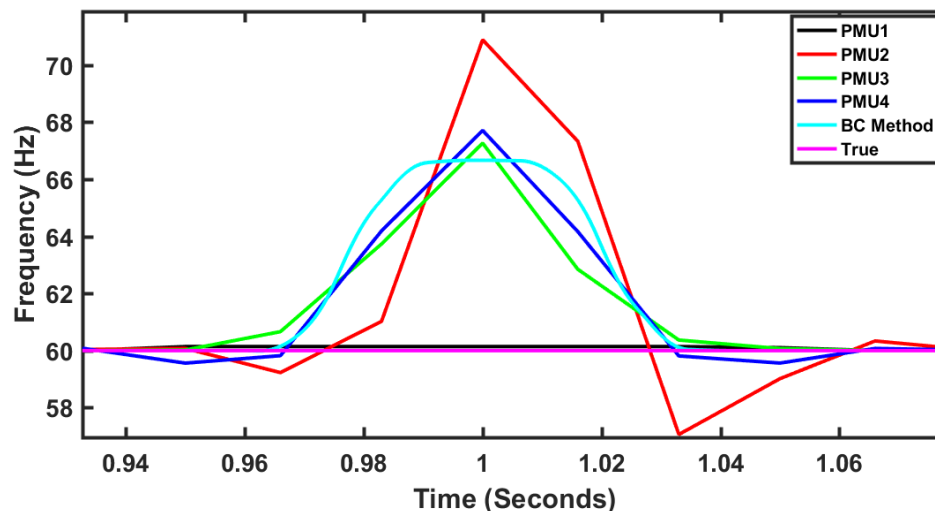
Figure 53: Phase angle input step at 90 degrees

The reported frequency error at one point is more than 70 Hz. As reviewed

earlier, under-frequency thresholds are set throughout the system to shed load. In this

case, it is an over-frequency condition, but had the input step been -90 as oppose to +90

degrees the measurement response would have been in the opposite direction. The PMU

could measure and report this condition as under-frequency and if the delay is not large

enough then the PMU would misidentify this as a frequency excursion. Under-frequency

time delays should be carefully considered due to this scenario.

A true power system frequency excursion was replayed through the PMUs and

during one reporting interval the PMUs reported nearly 750 mHz different. This

frequency event likely included a step-in phase angle, but this further illustrates the issues

of the reporting error.

5.2 Possible Future Work

The new method proposed for estimating power system frequency showed

promising results through testing. One main goal was to develop a simple and fast

frequency algorithm, this was achieved. Additionally, the PMUs responded very similar for many test cases, but there is area for improvements in the suggested areas:

- Improve the accuracy for the BC method during AM signal conditions

- Improve PMU responses throughout phase angle modulated signal conditions

- Large frequency error was reported throughout input step changes; consideration should be given for a validity check for the frequency measurement so that large error is not reported throughout for these conditions. For instance, the validity check could flag invalid reporting values such as when an input step is detected

- Agreement on a common definition for power system frequency

BIBLIOGRAPHY

[1]   B. Kasztenny, "What is Power System Frequency (email)," ed. Charlotte, 1/15/2015.

[2]   B. Kasztenny, "Definition of frequency in power grid Part II (meeting minutes)," ed. Atlanta, Georgia, 4/28/2015.

[3]   B. Kasztenny, "Definition of frequency in power grid Part I (phone meeting minutes)," ed. Charlotte, 2/17/2015.

[4]   H. Saadat, Power system analysis: WCB/McGraw-Hill, 1999.

[5]   A. G. Phadke and J. S. Thorp, Synchronized phasor measurements and their applications: Springer Science & Business Media, 2008.

[6]   "IEEE Standard for Synchrophasor Measurements for Power Systems," IEEE Std C37.118.1-2011 (Revision of IEEE Std C37.118-2005), pp. 1-61, 2011.

[7]   "IEEE Standard for Synchrophasor Measurements for Power Systems -- Amendment 1: Modification of Selected Performance Requirements," IEEE Std C37.118.1a-2014 (Amendment to IEEE Std C37.118.1-2011), pp. 1-25, 2014.

[8]   L. H. Fink, "Discrete events in power systems," Discrete Event Dynamic Systems, vol. 9, pp. 319-330, 1999.

[9]   N. Jaleeli, L. S. VanSlyck, D. N. Ewart, L. H. Fink, and A. G. Hoffmann, "Understanding automatic generation control," Power Systems, IEEE Transactions on, vol. 7, pp. 1106-1122, 1992.

[10]   "Overview of power system stability concepts," in Power Engineering Society General Meeting, 2003, IEEE, 2003, pp. 1-1768 Vol. 3.

[11]   J. A. Barnes, A. R. Chi, L. S. Cutler, D. J. Healey, D. B. Leeson, T. E. McGunigal, et al., "Characterization of Frequency Stability," Instrumentation and Measurement, IEEE Transactions on, vol. IM-20, pp. 105-120, 1971.

[12]   C. Concordia and L. H. Fink, "Load shedding on an isolated system," Power Systems, IEEE Transactions on, vol. 10, pp. 1467-1472, 1995.

[13]   B. Hoseinzadeh, F. Faria Da Silva, and C. L. Bak, "Power system stability using decentralized under frequency and voltage load shedding," in PES General Meeting | Conference & Exposition, 2014 IEEE, 2014, pp. 1-5.

[14]   S. S. Ladhani and W. Rosehart, "Under voltage load shedding for voltage stability overview of concepts and principles," in Power Engineering Society General Meeting, 2004. IEEE, 2004, pp. 1597-1602 Vol.2.

[15]   P. I. Obi, G. Chidolue, and I. I. Okonkwo, "PROTECTION AND CONTROL OF POWER SYSTEM-A REVIEW," 2014.

[16]   W. Tomasi, Electronic communications systems : fundamentals through advanced. Englewood Cliffs, N.J.: Prentice Hall, 1988.

[17]   B. Kasztenny, "A new method for fast freqeuncy measurements for protection applications," Schweitzer Engineering Laboratories, Inc., 20151112 2015.

[18]   A. G. Phadke and B. Kasztenny, "Synchronized Phasor and Frequency Measurement Under Transient Conditions," Power Delivery, IEEE Transactions on, vol. 24, pp. 89-95, 2009.

[19]   "IEEE Recommended Practice for Monitoring Electric Power Quality," IEEE Std 1159-1995, p. i, 1995.

[20]   E. Sorrentino and R. Carvalho, "Performance of three algorithms for frequency measurement under transient conditions," Electric Power Systems Research, vol. 80, pp. 1191-1196, 10// 2010.

[21]   S. Y. Xue and S. X. Yang, "Accurate and fast frequency tracking for power system signals," in Systems, Man and Cybernetics, 2007. ISIC. IEEE International Conference on, 2007, pp. 2754-2759.

[22]   M. S. Sachdev and R. Das, "Understanding microprocessor-based technology applied to relaying," Report of Working Group I-01 of the Relaying Practices Subcommittee, IEEE Power System Relaying Committee, 2009.

[23]   A. Abu-El-Haija, "Fast and accurate measurement of power system frequency," in Instrumentation and Measurement Technology Conference, 2000. IMTC 2000. Proceedings of the 17th IEEE, 2000, pp. 941-946.

[24]   T. S. Sidhu, "Accurate measurement of power system frequency using a digital signal processing technique," Instrumentation and Measurement, IEEE Transactions on, vol. 48, pp. 75-81, 1999.

[25]   R. V. Krishna, S. Ashok, and M. G. Krishnan, "Synchronised Phasor Measurement Unit," in Power Signals Control and Computations (EPSCICON), 2014 International Conference on, 2014, pp. 1-6.

[26]   A. G. Phadke, J. S. Thorp, and M. G. Adamiak, "A New Measurement Technique for Tracking Voltage Phasors, Local System Frequency, and Rate of Change of Frequency," Power Apparatus and Systems, IEEE Transactions on, vol. PAS-102, pp. 1025-1038, 1983.

[27]   R. G. Lyons, Understanding digital signal processing: Pearson Education, 2010.

[28]   W. Premerlani, B. Kasztenny, and M. Adamiak, "Development and Implementation of a Synchrophasor Estimator Capable of Measurements Under Dynamic Conditions," IEEE Transactions on Power Delivery, vol. 23, pp. 109-123, 2008.

[29]   "IEEE Standard Common Format for Transient Data Exchange (COMTRADE) for Power Systems," IEEE Std C37.111-1999, pp. 1-55, 1999.

[30]   OMICRON. (12/05). CMC 256plus Technical Data. Available: omicronenergy.com/fileadmin/user_upload/pdf/literature/CMC-256plus-Technical-Data-ENU.pdf

[31]   OMICRON. (12/05). CMIRIG-B Interface. Available: omicronenergy.com/fileadmin/user_upload/pdf/literature/CMIRIG-B-Technical-Data-ENU.pdf

[32]   S. E. Laboratories. (12/05). SEL-2407 Satellite-Synchronized Clock. Available: selinc.com/products/2407/